Current Pharmaceutical Design, 2008, *14*, 3854-3872

Subtype Selectivity in Phosphodiesterase 4 (PDE4): A Bottleneck in Rational Drug Design

P. Srivani[1], D. Usharani[2,3], Eluvathingal D. Jemmis[2,#] and G. Narahari Sastry[1,*]

[1]*Molecular Modeling Division, Indian Institute of Chemical Technology, Tarnaka, Hyderabad 500007, India;* [2]*Department of Inorganic and Physical Chemistry, Indian Institute of Science, Bangalore 560012, India;* [3]*School of Chemistry, University of Hyderabad, Hyderabad 500046, India and* [#]*Current address: Indian Institute of Science Education and Research - Thiruvananthapuram, CET campus, Thiruvananthapuram-695016, India*

Abstract: Subtype selectivity of phosphodiesterase 4 (PDE4) has been proposed to be the most salient feature for the development of drugs for asthma and inflammation. The present review provides an account of various strategies to overcome the side effects of the PDE4 inhibitors. Subtype selectivity and recent developments of molecular modeling approaches towards PDE4 were addressed using QSAR and docking, followed by a detailed structural analysis of more than three dozen available X-ray structures of PDE4B and PDE4D. Usually, the lack of a 3-dimensional structure of a target protein is a bottleneck for rational drug design approaches. However, in this case the availability of 39 X-ray structures along with co-crystals has not improved the therapeutic ratio of drugs through rational drug design approaches. The investigation of structures led to find significant variations in the M-loop region, which is the integral part of the active site of PDE4B and PDE4D. These differences can be accounted for by varying conformation of the Pro^{430} residue and a Thr^{436}/Asn^{362} mutation in the M-loop that causes variations in adjacent residue properties and also the pattern of hydrogen-bonding interactions. The impact of the M-loop region on inhibitor binding has been further scrutinized by MOLCAD surfaces and hydrophobicity. These have shown that PDE4B is more hydrophobic in nature than PDE4D in the M-loop region. A review of the above aspects given the emphasis on a new PDE4 inhibitor which can access both metal and solvent pockets may possibly lead to ligands with enhanced potency. The lining of the Q2 pocket that involves the M-loop region may be considered for the design of potent subtype-selective inhibitors.

Key Words: PDE4, asthma, subtype selectivity, rational drug design, molecular modeling, QSAR, docking, QM.

1. INTRODUCTION

In 1957, Sutherland and Rall reported phosphodiesterases (PDEs) as metallo-hydrolases which hydrolyze the phosphodiesterase bond of cyclic adenosine and guanosine 3',5'-monophosphates (cAMP and cGMP) to give the corresponding 5'-nucleotides (AMP and GMP) in various cells [1,2]. Thus, they regulate the levels of two second messengers, cAMP and cGMP, inside the cell which otherwise affect the specific protein phosphorylation cascades. Furthermore, these isozymes play a vital role in the regulation of various physiological functions such as visual response, smooth muscle relaxation, platelet aggregation, immune response, cardiac contractility, etc. [1-6].

There are more than 200 splice isoforms for 21 human PDE genes that encode for the 12 PDE isoenzymes [6]. The catalytic regions of the 12 known families of the cyclic nucleotide PDEs are well conserved. Each family exhibits >50% amino acid sequence identity within the conserved catalytic domain of about 250 residues, but sequence identity between different families is only 30-40%. The variations are mainly observed in the regulatory regions comprising the phosphorylation, cGMP binding and membrane insertion sites [3-5]. These isozymes also differ in their kinetic and physical characteristics, substrate selectivity, tissue distribution, subcellular localization, and sensitivity to endogenous activators and inhibitors [2, 3]. Based on their substrate specificity, these isozymes have been divided into three groups: a) cAMP specific (PDE4, 7 and 8), b) cGMP specific (PDE5, 6 and 9) and c) both cAMP and cGMP specific (PDE1, 2, 3, 10 and 11) enzymes. This enzyme family is much sought after as they are proved to be potential drug targets, such as PDE1 for atherosclerosis, PDE3 for cardiovascular disease, PDE5 for erectile dysfunction, etc. [7]. Among them, PDE4 is considered as a therapeutic target for the treatment of diseases like asthma, chronic obstructive pulmonary disease (COPD), allergic rhinitis, typeII diabetes, rheumatoid arthritis, etc. [8-12]. The interest arises both from the availability of inhibitors, which possess a significant degree of selectivity for one isozyme over others, and from the recognition of different PDE isozymes regulating cyclic nucleotide hydrolysis in different tissues.

Among the 12 PDEs, research on PDE4 and PDE5 has been particularly vigorous in recent years. However we would like to contemplate only the PDE4 family in our review. Identification and characterization of four different PDE4 subtypes along with their physiological importance has been achieved. An inclusive overview of aspects such as molecular biology, pharmacology, physiology and cell signaling exceed the scope of this review as a number of excellent reviews have already highlighted these important features [3-5, 8-15]. Nonetheless, molecular modeling ap-

*Address correspondence to this author at the Molecular Modeling Division, Indian Institute of Chemical Technology, Tarnaka, Hyderabad 500007, India; Tel/Fax: +91-40-27160512; E-mail: gnsastry@gmail.com

1381-6128/08 $55.00+.00

proaches towards the PDE4 family have not been sufficiently emphasized. Thus, in the current review we have mainly focused on recent progress in molecular modeling approaches applied to the PDE4 family. A detailed account of variations between the PDE4B and PDE4D protein structures and a brief discussion of what important features have to be considered to design new PDE4 drug candidates are presented.

2. SIMPLICITY AND COMPLEXITY OF PDE4 AS A DRUG TARGET

Success in selecting any protein or other biomolecule (DNA/RNA) as a drug target depends on how simple the inhibiting/activating mechanism of the macromolecule is. This in turn relies on the availability of information on aspects such as the biochemical cascade in a disease, the physiological role of that particular biomolecule of interest in that cascade and the ease of obtaining the tertiary structure (or sequence). Furthermore, knowledge of details of the substrate binding site and (or) the presence of other binding (allosteric) sites are also crucial to inhibitor design. In this concern, PDE4 appears to be a very advantageous target because of its well explored physiological role (importance in signal transduction), tissue distribution (ubiquitous presence of 4 subtypes), availability of a range of crystal structures (>30) and lastly the information about the substrate (cAMP) binding site [14, 15]. However, the existence of high sequence similarity (>80%) of the catalytic domain among the subtypes makes PDE4 as very complex target to design a drug. Similarities in the catalytic domains of the PDE4 subtypes force most of the inhibitors to be nonselective. Other reasons which make PDE4 a complicated target are discussed in the subsequent sections 2.3 and 2.4 (Subtype selectivity and other strategies to overcome side effects).

2.1. Structure and Expression

PDE4 is a cAMP specific PDE that is coded by four distinct genes A, B, C and D. The mRNA splicing of these genes further generates 22 splice variants (Table **1**). All the PDE4 isoforms (splice variants) can be divided structurally into three major categories as long, short and super short forms based on upstream conserved regions (UCR1 and UCR2) [13,14]. Each of these four genes is characterized by its regulation, subcellular localization and protein-protein interactions [16-18]. PDE4A, 4B and 4D are expressed in inflammatory cells, namely eosinophils, T cells, B cells, neutrophils, etc., whereas the expression of PDE4C is low (Table **1**) [19, 20]. The wide distribution amongst inflammatory cells in humans led to the idea that their selective targeting might be an approach for the inhibition of eosinophils and T lymphocytes in asthma and the inhibition of neutrophils and CD8+ T lymphocytes in COPD [21, 22].

2.2. Inhibitors and Causes of Side Effects

Theophylline, a PDE inhibitor, has been used for the treatment of asthma for last few decades. The non-specificity of this drug causes a range of gastrointestinal, central nervous and cardiovascular side effects [23, 24]. This suggests the need of a specific PDE4 inhibitor as potential drug for asthma on the basis of its tissue distribution. Rolipram has been reported as the first selective PDE4 inhibitor. There are various classes of novel orally active PDE4 inhibitors. Based on their structural motifs, PDE4 inhibitors can be broadly classified into three categories as xanthines, catechol ethers and heterocyclics (nitraquanzone, benzofurans, indoles, isoquinoline, pyridopyrimidinones, pyrazolopyridines, etc.). The details of the analogs are not discussed here as they have been well reviewed earlier [25-28]. The first generation PDE4 inhibitors like rolipram, RO-20-1724 (mesopram) and zardaverine discarded in clinical trails due to side effects like nausea, vomiting, dyspepsia, and headache [8]. The second-generation rolipram analogs (cilomilast, roflumilast and the most potent piclamilast) are now in phase III clinical trials. However, they have also suffered from low therapeutic ratios [29]. The details of clinical trails for the various PDE4 inhibitors are reviewed in references 30-34.

The possible reasons for the side effects of the inhibitors are a) existence of two conformational states of PDE4, described as low-affinity (LA) and high-affinity (HA) forms [35], where the high-affinity conformation is stated to cause side effects [36-38]; b) poor blood brain barrier (BBB) regions in the emetic centers of the central nervous system (CNS) allowing circulating drugs to be absorbed easily and cause emesis [28]; c) the area postrema and the nucleus tractus solitarius are the emetic regions in CNS that profoundly express the PDE4D subtype (Table **1**) [39]. This raises the cAMP levels in gastric secreting cells in the gut, resulting in emesis. In order to minimize the side effects various strategies have emerged in recent years and are summarized below.

2.3. Subtype Selectivity

Among the strategies to reduce the side effects, subtype selectivity appears to offer extensive opportunities for pharmacological intervention directing drugs to a remedial target for developing next generation PDE4 drugs [19, 30, 40, 41]. In this review we will highlight the evidence and the inhibitors that have shown some subtype specificity.

The first evidence about subtype selectivity arouse from investigations on a range of second-generation PDE4 inhibitors (cilomilast, roflumilast) that have weak subtype selectivity. The study led to the understanding that inhibitors with selectivity for 4A/4B enzymes would be more effective than those selective for 4D [42]. PDE4C is precluded as a potential target since it is not expressed in inflammatory and immune cells. Even though PDE4C is present in the lung epithelium its mechanism is not very clearly understood [28]. In addition to this, gene knockout studies on mice have provided crucial evidence to explain the physiological role of the PDE4B and 4D subtypes [43]. 4D deficient mice were predicted to have an inflammatory response but not airway hyperreactivity when exposed to allergen due to a lack of cholinergic stimulation of muscarinic receptors [44]. On the other hand, in 4B deficient mice induced PDE4 activity was absent on lipopolysaccharide stimulation (LPS), and this was not significantly affected in the case of 4D deficient mice [45]. This is because in the 4B wild type, LPS induces an increase in 4B mRNA levels in both human monocytic THP-1 cells and in circulating leukocytes. The 4B knock-out mice also showed reduced duration of action of xylazine/

Table 1. Classification of Isoforms and Tissue Distribution of PDE4 Subtypes

S. No	Characteristics	PDE4A	PDE4B	PDE4C	PDE4D
1.	Splice variants	5	4	3	9
	Long	A4B, A8, A10	B1, B3, B4	C1, C2	D3, D4, D5, D7, D8, D9
	Short	–	B2	–	D1
	Super short	A1	–	–	D2, D6
2.	Liver, Kidney, Placenta, Neuroblastoma (SH-SY5Y) and Heart	++	++	++	++
3.	Skeletal muscle	+++	+++	+++	+++
4.	Testis, ovary and small intestine	+	+	+	+
5.	Colon	+	+	ND	++
6.	Spleen	+	++	–	+
7.	Lung, Trachea,	++	++	++	++
8.	Neuroblastoma (SK-N-SH)	++	++	±	++
9.	B-like, Promyelocytic	++	++	–	–
10.	Blood, Eosinophils, Promonocyte-like	++	++	–	++
11.	Retinoblastoma	++	–	±	–
12.	Neutrophils	±	++	–	±
13.	T-like Th1 Th2	++ ++ ++	– ++ ++	–	– – ++
14.	Lung carcinoma	±	–	–	++
15.	Brain Area postrema, Nucleus tract solitaris	–	+	–	++
16.	Macrophage	++	–	–	–
17.	Parietal cells, Nodose ganglion	–	–	–	++

+++ strong expression; ++ expression; ± weak expression; – no expression;

ketamine, which triggers anesthesia and is used as a surrogate marker for emesis in mice that usually demonstrate vomiting [46]. The gene knock-out studies extrapolate to the conclusion that side effects will be reduced upon 4B inhibition over 4D.

Earlier studies reported that a truncated 4A and fully recombinant 4B exist in the high affinity rolipram binding state (HARBS). However, two subtypes have shown K_d values between 1 and 5 nM, respectively [47]. Additional studies on smokers and nonsmokers gave evidence of up-regulation of PDE4A4 in lung macrophages and both 4A4 and 4B2 in peripheral monocytes in smokers [48]. Chronic treatment with proinflammatory mediators also regulated the 4B2 isoform in monocytes [49]. Among the 4A and 4B, the short isoform of 4B (PDE4B2) is most commonly expressed and is activated by ERK phosphorylation stimulation of inflammatory cells, and not 4A, as it does not have any short splice variants (Table **1**) [13, 14, 16]. Therefore, biochemical and structural biology explain clearly that selective targeting of PDE4B is advantageous over the other subtypes. This implies the necessity for the design of subtype selective inhibitors.

The first known subtype selective inhibitor is cilomilast, that has shown 10-fold selectivity towards the 4D subtype [29, 50, 51]. Later, a novel nicotinamide series [26] and 6,8-disubstiuted 1,7 napthyridines [52], L-454-560 have been reported as potent 4D subtype selective molecules [53]. High potency towards 4D is due to phosphorylation by cAMP-dependent protein kinase A, and the fact that the phosphorylated 4D enzyme is much more sensitive to such inhibitor

structures [54]. The known inhibitors that are slightly selective towards 4B are ibudiblast [55] and pyrrolo[2,3-d]pyri-"dazinones [56]. No leads are not yet known that are highly selective towards 4B.

2.4. Other Strategies to Overcome the Side Effects

Ample numbers of reviews and research articles published in the last 3-4 years explained some other strategies to reduce these side effects [30, 40, 50]. Excluding subtype selectivity, strategies that can also possibly reduce side effects are discussed below.

2.4.1. Inhibitors Selective for Low Affinity Versus High Affinity Forms

The existence of two conformational forms of PDE4 in HA and LA rolipram binding states has led to the idea of developing low affinity rolipram binding drugs. The second-generation inhibitors, namely roflumilast, piclamilast and cilomilast, have been shown to have similar binding affinity towards high and low affinity PDE4 conformers. Various inhibitors like DHPQ (dihydropyrazolo[4,3-c]quinolin-3-one), benzofurans and AWD-12-281 are reported to show relative selectivity for low affinity form of the enzyme, but still had minimum emetic potential [26]. Therefore, not all anti-inflammatory effects and side effects of the PDE4 inhibitors are mediated through the low affinity rolipram binding site conformation. This simplistic hypothesis is now no longer exploited in compound development.

2.4.2. Drugs with Low BBB Permeability

Reduced lipophilicity of inhibitors possibly will allow the development of drugs with low BBB permeability. This hypothesis also has a disadvantage as the active site is more lipophilic in nature (Q1 and Q2 pocket) and so inhibitors may lose specificity towards the PDE4 protein [57]. It was suggested that interactions of the lipophilic moiety of rolipram and its analogs with the Q1 and Q2 pockets play a crucial role towards PDE4 selectivity over other cAMP specific PDE7 and PDE8 proteins [58, 59].

2.4.3. Disease-Activated Drugs

Disease-activated drugs (DAD) are drugs which are directly released in the diseased area. These drugs can be used in combination with a steroid or other active compound that can form a covalent linkage [24]. The drug combinations are inactive as such and need to be activated in the target tissue by a disease specific mechanism (e.g., proteolytic enzymes, free radical mediators, alteration in local pH or redox potential), specifically in inflamed tissues [60]. This approach could potentially improve the therapeutic window and therefore amend the pharmacokinetics. Until now isoquinoline derivatives, as inhaled PDE4 inhibitors, have been reported to function as DAD in combination with corticosteroids (dexamethasone and budesonide) [60].

2.4.4. Dual Inhibitors

The dual inhibitor strategy is a rather novel approach to target more than one protein while satisfying the obligation that both proteins ought to be involved in the same physiological cascade. The main intention behind the dual inhibitors is to enhance efficacy and eliminate off-target effects [61]. Targeting a combination of PDE 3, 4, 5 and 7 has emerged recently based on their cellular distribution [62]. The dual PDE3-4 inhibitor may provide more bronchodilator and bronchoprotective effects, while a dual PDE4-5 combination may possibly have beneficial effects on hypoxic pulmonary hypertension and vascular remodeling [50]. The tissue distribution urges the possibility of a dual PDE4-7 inhibitor, which may be more effective for asthma and COPD [63, 64]. Among the three PDEs that can function as dual targets with PDE4, PDE7 appears to be superior in terms of isolation, characterization and tissue distribution [65, 66]. Specific PDE7 and PDE4-7 inhibitors are emerging now [67, 68].

In addition to the reasons mentioned in the foregoing discussion, subtype selectivity appears to be a key strategy, albeit very subtle, in lead optimization. Now it is time to have a keen look at the various computational approaches established for the PDE4 family.

3. MOLECULAR MODELING APPROACHES

There are various computational chemical approaches such as docking, quantitative structure activity relationships (QSAR), homology modeling, QM/MM [69-72], molecular dynamics (MD) simulation [69,72,73] and virtual screening [74], which added to combinatorial chemistry [74b] are playing an important role in drug discovery and to understand disease mechanisms. In the year 1999, before crystallization of the first PDE4 protein, a peptide binding site model was reported by Polymeropoulos *et al.* [75]. This binding site model consists of five amino acid residues (two tryptophans, one each of tyrosine, histidine and asparagine), Zn^{2+} and an envelope of charged virtual particles that were constructed by taking 21 diverse PDE4 inhibitors (rolipram, nitraquazone, xanthine derivatives, imidazopyridopyrazinones, 5-oxyindoles). The model proposed that there are three hydrogen bonding interactions contributing to the inhibitors. These are: 1) tryptophan residues donating to the alkoxy oxygen atoms of the rolipram and pyridopyrazinone analogues or to the nitrogen atoms of the xanthine derivatives, 2) the tyrosine residue donating to the imidazo nitrogen of the pyridopyrazinones and 3) the histidine residue donating to the carbonyl oxygen atoms of LAS, RPR, GW3, pyridopyrazinones and 5-oxyindoles. The model also suggested an electrostatic site, possibly through a Zn atom [75]. Based on the above study, in the year 2002, Richter *et al.* identified a few residues involved in the inhibitor binding of PDE4 using site-directed mutagenesis techniques [76]. These studies ruled out the participation of tryptophan in the hydrogen bonding and supported the relevance of hydrophobic interactions. However, the X-ray structures reported in the subsequent years showed that it is a glutamine residue and not tryptophan which donates hydrogen bond to an alkoxy oxygen atom of rolipram and to a nitrogen atom of the xanthine derivatives, respectively. Also, tyrosine, histidine and to some extent tryptophan residues have been suggested to play an important role in substrate binding and for structural stabilization of the protein. Albeit the peptide model was not very successful in suggesting the correct residue involved in the interaction (Trp or Gln), it was able to propose a few potential interactions for the first time. On the other hand, site directed mutagenesis studies had demonstrated the im-

portance of some residues (Asp^{241}, His^{390}, His^{433}, His^{437}, Phe^{414}, Phe^{446}, Pro^{396}, Trp^{406} and Tyr^{403}) that are involved in substrate specificity as well as in inhibitor specificity [76-82]. In the absence of a crystal structure, comprehensive mutagenesis studies and the peptide model initially provided the basic idea of the active site and probable protein-ligand interactions. Among the various molecular modeling approaches such as QM/MM [69-72], MD [69, 72, 73] and virtual screening [74a] we will confine our discussion to analog and structure-based approaches namely QSAR and docking in the subsequent sections.

3.1. QSAR

In order to minimize expensive drug failures it is essential to determine the potential biological activity of new candidates as early as possible. In this perspective, computer-aided rational drug design strategies like QSAR and docking approaches have emerged as promising tools [83-86]. Ample numbers of SAR studies on various heterocyclics, namely pyrazolopyrimidines, quinolines, benzodiazepines, benzofurans, furopyridinecarboxamides, oxazoles, thiadiazines and catechol diethers, catechol hydrazines and cyclohexane rings as PDE4 inhibitors have been reported [87-94]. However, *in silico* approaches using traditional QSAR applications in the development of the new PDE4 inhibitors are meager.

In the year 2003, a couple of 3D-QSAR studies on PDE4 inhibitors, namely heterocycles like thieno[3,2-d]pyrimidines and indole derivatives, were reported [95, 96]. These studies suggested that sterically demanding substituents on pyrimidine and indole rings are not very favorable whereas electronegative groups that may readily interact with the metals are favorable. Possibly, a complementary structure-based analysis like docking along with QSAR might provide more information in terms of available active site space and crucial protein-ligand interactions [84-86]. Two of the current authors have reported a combined application of 3D-QSAR and complementary molecular docking on triarylethane analogues as PDE4 inhibitors [84]. That study suggested substitution of electronegative groups on the pyridine ring, as docking studies had shown the pyridine moiety orienting towards the metal pocket. The combined QSAR and docking analysis revealed hydrogen bonding interactions between amide side chains and His^{164}, Asp^{201}, Thr^{271} and Asp^{318} besides Gln^{369} exhibit hydrogen bonding interactions with alkoxy groups. Another important finding of the study was the possibility of pyridine nitrogen protonation under physiological conditions being prevented by means of N-oxide formation. The SAR study on compound L-791,943, in which the nitrogen atom of the pyridine is replaced by nitrogen oxide, has supported the above observation [97].

3.2. Docking

Molecular docking is widely used to predict the binding orientation and binding affinity of new ligands for molecular targets [98]. Along with other factors, success of a docking study also depends on the quality of the scoring function used. An imperfect scoring function can mislead by predicting incorrect ligand geometries or by selecting nonbonding molecules over true ligands. The first crystal structure solved was the PDE4B catalytic domain [99], and molecular docking studies on this structure with cAMP and rolipram have allowed some rational understanding of the protein-ligand interactions [100]. Further increase in the number of crystal structures in the PDB with various other inhibitors explained the strong interactions in the active site of the protein. A class of nitroquinazone analogs along with rolipram was explored to analyze key protein-ligand interactions and it was found, based on the EZ conformer, that it has different hydrogen bond acceptor regions compared to other reported PDE4 inhibitors [101]. In 2005, the efficiency of the docking program (Ligand Fit) and the behavior of the selected scoring functions were thoroughly investigated using a high quality data set of PDE4B inhibitors [102]. Later an empirical free energy model was employed on PDE4 inhibitors to explore their biological activity [103]. The variance of estimated binding energy in this set is 0.68. The IC_{50} for each active and inactive compound was uniformly determined [103]. The MD calculations were also performed on the PDE4B and 4D isoforms. PDE4D co-crystallized with rolipram was used to verify the docking performance in order to identify the bioactive orientation of a PDE4 inhibitor. Lawrenz *et al.* have also applied the docking protocol on a completely different scaffold of PDE4 inhibitor (EMD 94360 and 95382) and estimated the binding affinities [104a]. The docking poses of these ligands have shown key hydrophobic interactions with Phe^{446} and Ile^{410}. The three side chains of amino acids Leu^{393}, Met^{347}, and Asp^{346} have shown contacts or proximity to the central pyridazinone ring of the ligands. Instead of pointing to a metal pocket, the long tail of the ligand is located in the solvent pocket (Pro^{430}, Ser^{282}, Asn^{283} and Gln^{284}) [104a]. The zardaverine analogs that were obtained through combinatorial chemistry were further explored using docking studies [74]. 2,1,3-Benzothiadiazine derivatives with a 3,5-di-tert-butyl-4-hydroxybenzyl moiety at the N1 position were found to be active and selective at the micromolar level towards PDE4, and the molecular modeling studies predicted that the increase in activity is due to occupation of a solvent sub-pocket [104b]. The new analogues have shown similar interactions to those of zardaverine with the protein; also the extension of alkyl chain length up to five carbons leads to the optimum biological activity as the pocket next to the metal site is more utilized. The last section emphasizes the crystal structures.

3.3. Crystal Structure Analysis

In this section, we would like to rationalize the structural requirements of PDE4 to attain subtype selectivity, by a comparative analysis of the available PDE4 crystal structures. About 60 X-ray crystal structures have been deposited for the PDE family in these 10 years. These crystal structures explain the substrate and inhibitor selectivity between each class of the family [30, 40, 105, 106]. In the case of PDE4, there are a total of 17 solved X-ray crystal structures for 4B and 20 for 4D deposited so far in the PDB (Table **2**). Among the 4B crystal structures, one PDB entry (1F0J) represents the uncomplexed protein and the other 16 correspond to co-crystals [57-59, 99, 107-113] with various PDE4 inhibitors (Table **2**). However, to our knowledge, the experimental structure of the uncomplexed 4D structure is not yet available. There is one each for PDE4 subtypes with NPV inhibitor that have been deposited recently [107].

Table 2. The Details of Ligand Name, PDBID (PID), Resolution (R), Type of the Secondary Structure (SS) and pH Maintained in the Crystallization Conditions for Available X-Ray Crystallographic Structures of PDE4 Subtypes (PST)

S. No	PST	PID	R (in Å)	Ligand Name	pH	SS	Crystallization Conditions
1	A	2QYK	2.10	NPV	8.5	Turn	12% PEG400, 200 mm Mg acetate, 0.1m Tris HCl pH 8.5, 5% glycerol,
2	B	1F0J	1.77	-	7.0	Turn	PEG
3	B	1ROR	2.00	cAMP	6.5	Turn	PEG 3000, sodium acetate, glycerol, sodium cacodylate,
4	B	1RO6	2.00	Rolipram			
5	B	1RO9	2.13	8-Br AMP			
6	B	2QYL	1.95	NPV	8.5	Turn	12% PEG3350, 0.1m Tris HCl pH 8.5, 35% ethylene glycol, 200 mm $MgCl_2$,
7	B	1TB5	2.15	cAMP	10.0	3_{10}-helix	Ammonium sulfate, lithium sulfate
8	B	1XMY	2.40	Rolipram			
9	B	1XN0	2.31	R,S rolipram			
10	B	1XLX	2.19	Cilomilast			
11	B	1XM4	2.31	Piclamilast			
12	B	1XMU	2.30	Roflumilast			
13	B	1XLZ	2.06	Filamilast			
14	B	1XM6	1.92	R-Mesopram			
15	B	1XOS	2.28	Sildenafil			
16	B	1XOT	2.34	Vardenafil			
17	B	1Y2J	2.55	Pyrazole			
18	B	1Y2H	2.40				
19	C	2QYM	1.90	NPV	7.5	Turn	10% PEG 3350, 100 mm $MgCl_2$, 0.1m Hepes pH 7.5
20	D	1PTW	2.30	cAMP	7.50	Turn	50 mm Hepes, 15% PEG 3350, 25% Ethylene Glycol, 5% Methanol, 5% DMSO
21	D	2PW3	1.56	cAMP	7.50	Turn	0.1 M HEPES, 0.1M $MgCl_2$, 12% PEG3350, 30% Ethylene Glycol, 10% Isopropanol
22	D	1TB7	1.63	cAMP	7.00	Turn	PEG 3000, ethylene glycol, isopropanol, glycerol, DTT
23	D	1TBB	1.60	Rolipram			
24	D	1Q9M	2.30	Rolipram	7.50	Turn	0.1 M HEPES, 20% PEG3350, 30% Ethylene Glycol, 10% Isopropanol, 5% Glycerol
25	D	1OYN	2.00	R,S-Rolipram	7.50	Turn	50 MM HEPES, 20% PEG3350, 25%Ethylene glycol, 20% Isopropanol
26	D	1XOM	1.55	Cilomilast	7.0	Turn	PEG3350, Ethylene Glycol, Isopropanol, Glycerol and DTT
27	D	1XON	1.72	Piclamilast			
28	D	1XOQ	1.83	Roflumilast			
29	D	1XOR	1.54	Zardevarine			
30	D	1MKD	2.90	Zardevarine	6.5	Turn	PEG8000, Mg acetate, DTT,
31	D	1RKO/1ZKN	2.10	IBMX	7.50	Turn	0.1M HEPES, 20% PEG 3350, 30% Ethylene Glycol, 10% Isopropanol, 5% Glycerol

(Table 2) contd....

S. No	PST	PID	R (in Å)	Ligand Name	pH	SS	Crystallization Conditions
32	D	1Y2B	1.40	Pyrazole	7.0	Turn	PEG3350, Ethylene Glycol, Isopropanol, Glycerol and DTT
33	D	1Y2C	1.67				
34	D	1Y2D	1.70				
35	D	1Y2E	2.10				
36	D	1Y2K	1.36				
37	D	2FM0	2.00	L-869298	7.50	Turn	0.1 M HEPES, 15% PEG3350, 25% Ethylene Glycol, 5% Isopropanol, 5% Glycerol
38	D	2FM5	2.03	L-869299	7.50	Turn	0.05 M HEPES, 15% PEG3350, 25% Ethylene Glycol, 5% Isopropanol, 5% Glycerol
39	D	2QYK	1.57	NPV	7.50	Turn	8% PEG3350, 0.1 HEPES PH 7.5, 30% Ethylene Glycol, 10% isopropanol, 200mm $MgCl_2$

3.3.1. Primary, Secondary and Tertiary Structural Differences

In general, the structural disparities between similarly functioning proteins arise either by mutation of an amino acid or by changes in its conformation, which in turn depend on surrounding residues through an intricate network of hydrogen bonding and other non-bonded interactions. Hence, to unravel these differences, structural alignment of all 4B and 4D structures with identical ligands is done and the resultant variations are analyzed below.

3.3.1.1. Sequence Differences

The sequence alignment of the 4B and 4D catalytic domains shows a similarity of 75-80% as reported earlier [14]. All the residues that interact with the metal and the cAMP are absolutely conserved between the two subtypes (Fig. **1**). A total of 49 residues are mutated between the two sequences (Fig. **2**), 30 of which are found in helices 1, 2, 3, 4, 5, 16 and 17 including the loop regions that are located in the N- and C- terminals. At the same time, helices 8, 9, 10 and 15 and the loop region of helix12/13, which is also known as

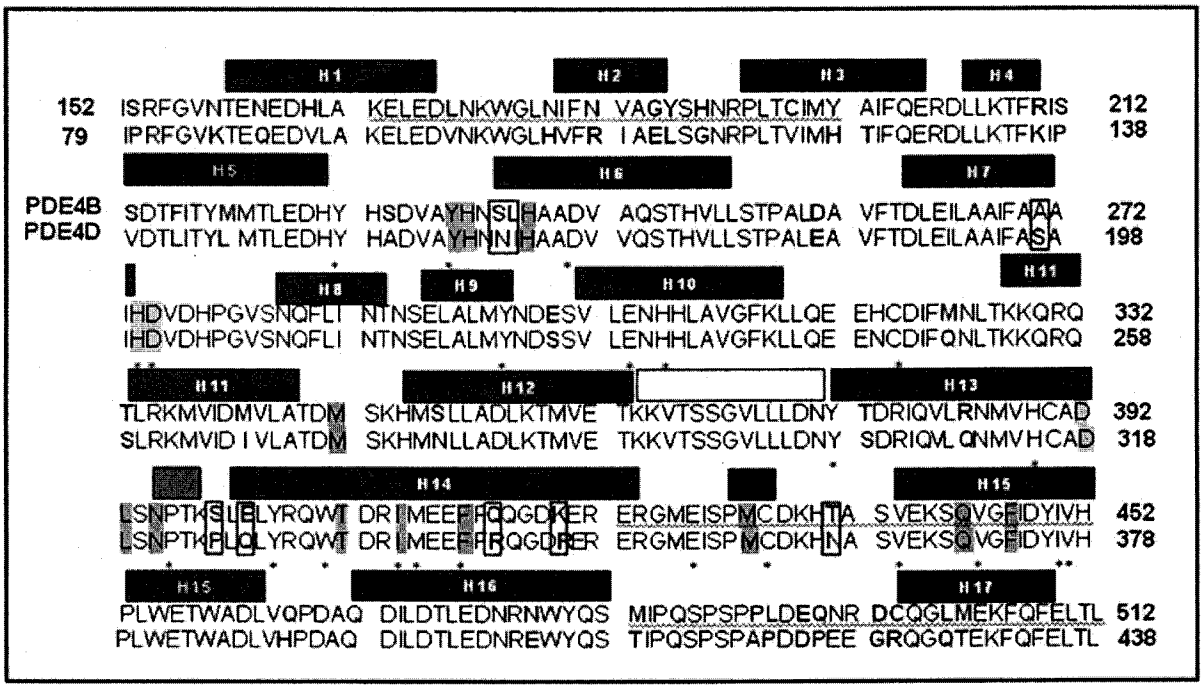

Fig. (1). Sequence comparison of PDE4B and 4D catalytic domains where the horizontal bars represent helices (numbered), β-hairpin (between H12 and H13), 3_{10}-helix and turn (between H13, H14 and H15). Residues that are interacting with the metal ions and ligands are grey shaded. * represents site directed mutagenesis studied residues. Mutated residues are shown in bold and lastly, the boxes represent mutated residues that are near the active site pocket.

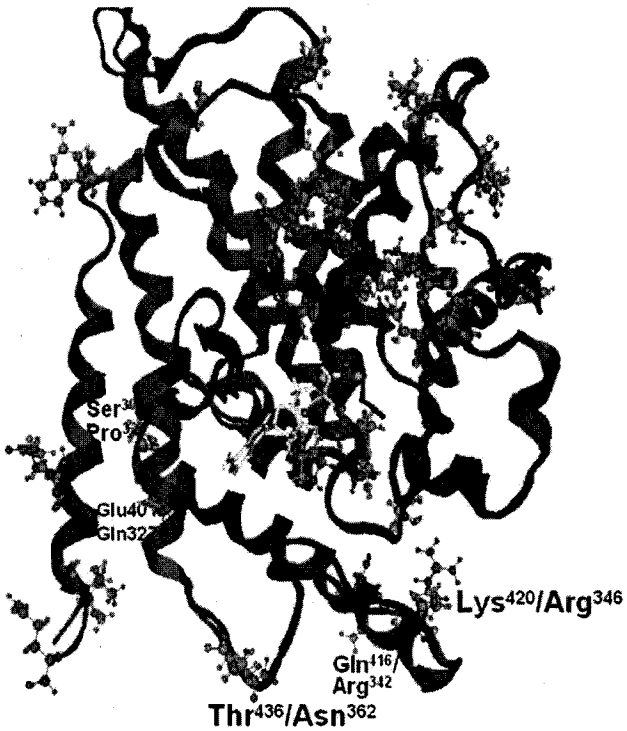

Away from the active site pocket	Near the active site pocket
Ser^{229}/Ala^{155}	Ser^{236}/Asn^{162}
Ala^{243}/Val^{169}	Leu^{237}/Ile^{163}
Asp^{256}/Glu^{182}	Ala^{271}/Ser^{197}
Glu^{300}/Ser^{226}	Ser^{399}/Pro^{325}
His^{319}/Asn^{245}	Glu^{401}/Gln^{327}
Met^{324}/Gln^{250}	Gln^{416}/Arg^{342}
Thr^{333}/Ser^{259}	Lys^{420}/Arg^{346}
Met^{341}/Ile^{267}	Thr^{436}/Asn^{362}
Ser^{352}/Asn^{278}	
Thr^{378}/Ser^{304}	
Arg^{385}/Gln^{311}	
Gln^{463}/His^{389}	
Asn^{478}/Glu^{404}	

Fig. (2). The protein tertiary structure is represented in helices and loops. The secondary structure variation in the M-loop region is displayed as a helix. The mutated residues are shown as ball and stick models. The stick rendering represents the ligand cAMP and balls represent metal atoms Zn and Mg. The table shows mutated residues in the catalytic domain of 4B and 4D that are located away from and close to the active site.

the extracellular regulatory kinase (ERK) docking site, are entirely conserved. The remaining 19 mutated residues are distributed in the remaining helices and also in the loop regions. Among them, only eight residues lie near the active site pocket.

Among these eight, the first three residues, Ser^{236}/Asn^{162}, Leu^{237}/Ile^{163} and Ala^{271}/Ser^{197}, are located near the metal binding pocket. Next two Ser^{399}/Pro^{325} and Glu^{401}/Gln^{327} are positioned in a 3_{10}-helix that exist between helix 13/14 and almost face the surface of the protein. The last two residues are Gln^{416}/Arg^{342} and Lys^{420}/Arg^{346}, present in helix 14 that has mostly hydrophobic residues and lie near the bottom of the active site pocket. The most interesting residue is Thr^{436}/Asn^{362}, situated in the M-loop region (424-437), which is an integral part of the active site hydrophobic pocket (Fig. **2**). The varied hydrogen-bonding pattern with neighboring residues because of this mutation makes it interesting to study further and is discussed in the following sections.

3.3.1.2. Turn vs 3_{10}-Helix

According to Xu *et al.* [99], there are 17 α helices and one β hairpin in the 4B structure. 16 α helices and β hairpin are also observed in the 4D structure, with an exception of the three and half residues (Ser^{429}, Pro^{430}, Met^{431} and Cys^{432} – the numbering corresponds to the 4B structure) of the M-loop region that exist as a 'turn' in 4B and 4D and as a '3_{10}-helix' in some of the 4B (Fig. **3**). A broad insight of the two classes of 4B differing in secondary structure (3_{10}-helix versus turn) is shown in Table **2**. We contemplate the possibility that the turn/3_{10}-helix switch over may have a significant impact on the active site and thereby the function of the protein. Nonetheless, the flexibility of this loop region upon ligand binding has been discussed earlier [58, 59], but no attention seems to have been paid to the important secondary structure alteration. This type of alteration has been reported to be important recently in the PDE5 crystal structure where under the influence of ligand binding there are secondary structural alterations [114].

The superimposition of the Cα atoms of 4B, having a '3_{10}-helix' (Fig. **3a**), with those of 4D and 4B having a 'turn' over 4D (Fig. **3b**), reveals that the two subtypes mainly differ in three loop regions of helices 10/11, 12/13 and 14/15 (4B deviates 0.66-0.67 Å from 4D). The former two are involved in protein-protein interactions with UCR1 and UCR2 and the KIM docking site for extracellular signal-regulatory (ERK) kinase [14] and the latter one, which is known as the M-loop, is important for inhibitor selectivity [58, 59].

3.3.1.2.1. Reasons for Secondary Structure Alteration

According to standard protein structure rules, three and a half residues are required per turn of α-helix where the carbonyl oxygen atom of the first residue forms a hydrogen bond with the hydrogen atom of fourth residue's nitrogen. In 4B 'helix' forming structures (in the M-loop), the backbone CO group of Ser^{429} forms a hydrogen bond with 'NH' group of Cys^{432} and the backbone CO group of Pro^{430} forms another hydrogen bond with the NH group of Asp^{433}. The two hydrogen bonds lead to have a'3_{10}-helix like' secondary

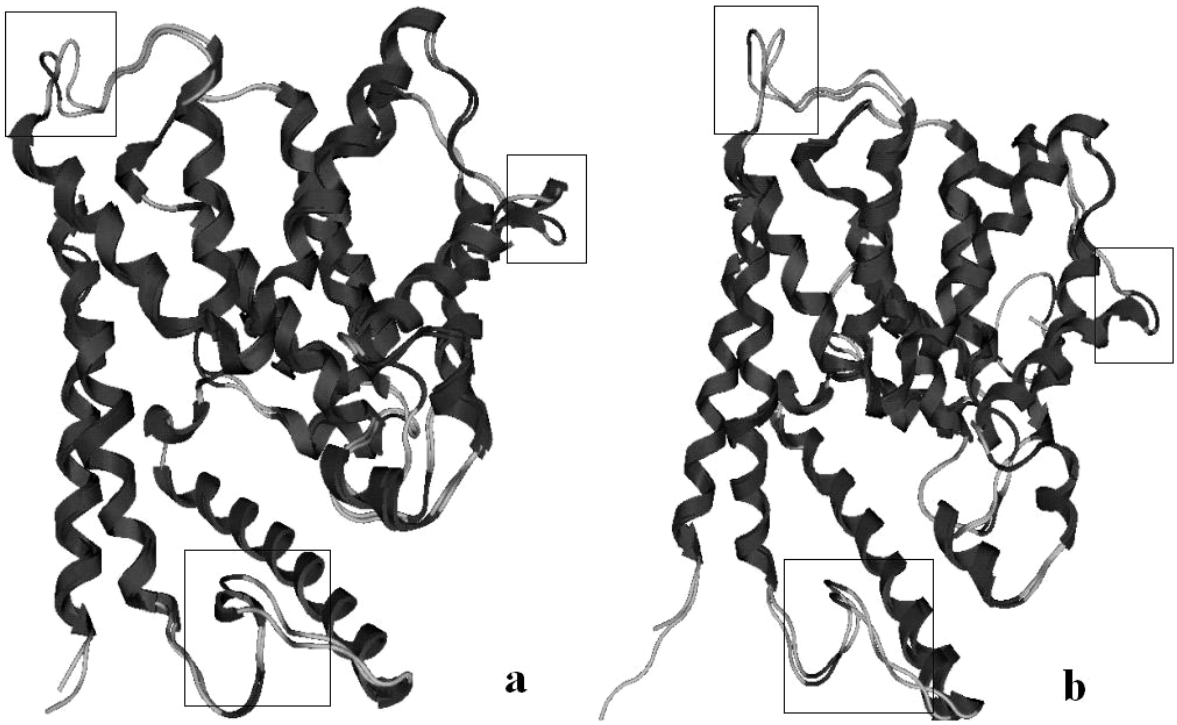

Fig. (3). Superimposition of the tertiary structures of PDE4B and 4D **a)** The 4B structure that has a '3_{10}-helix' in the M-loop region is overlaid on 4D and **b)** The 4B structure having a 'turn' in the M-loop region is posed on 4D. The three varying regions are highlighted in the black boxes.

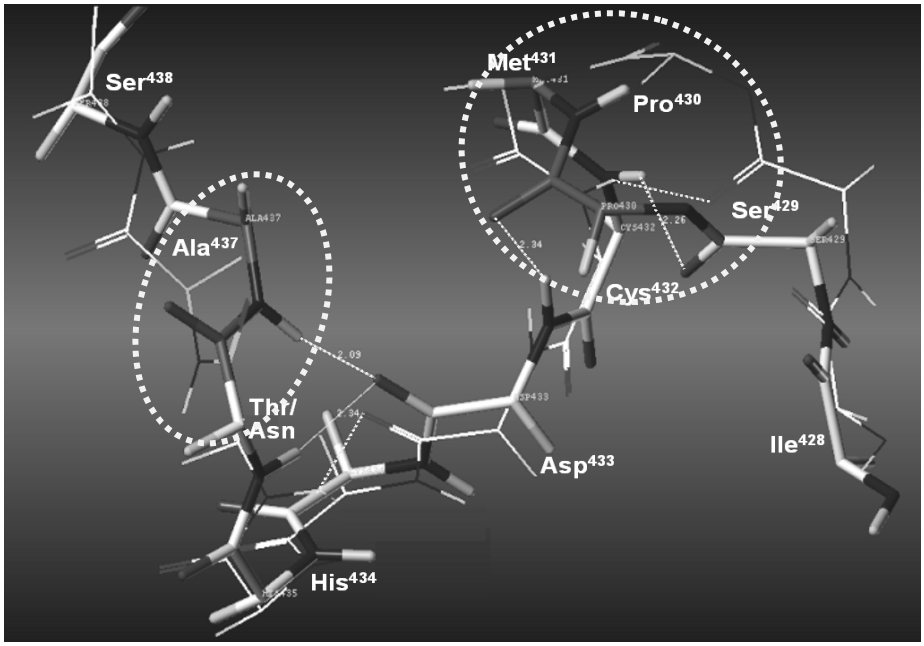

Fig. (4). Variation in the hydrogen-bonding pattern of the M-loop due to Thr/Asn mutation as shown in PDE4B and 4D. The amino acid residues are displayed in capped sticks (4B) and in lines (4D) whereas the hydrogen bonds are represented as dotted lines. The change in dihedral angles of the backbone because of a mutated residue is highlighted in dotted ovals.

structure in 4B whereas in 4D the similar hydrogen bonding pattern was not observed (Fig. 4). The Thr^{436}/Asn^{362} mutation that was found near the M-loop was thought to be the reason for the secondary structure adaptation. In 4B, the Thr^{436} residue that is adjacent to the Ala^{437} residue changed the orientation of the alanine side chain in such a way that it could form hydrogen bonds with Lys^{434} and Asp^{433}. Asp^{433} in turn formed a hydrogen bond with Pro^{430} resulting in a backbone alteration of Pro^{430}. The adjacent Ser^{429} residue forms a hydrogen bond with Cys^{432} favoring the '3_{10}-helix like' structure (Fig. 4). Conversely, in 4D, Asn^{362} is present in place of Thr^{436} and positions the alanine side chain with a different dihedral angle and even the orientation of Pro^{356} is changed and hence is not able to form hydrogen bonds as observed in 4B. Instead of two hydrogen bonds seen in '3_{10}-helix' structures, only a serine residue hydrogen bond is retained in 4D structures which thus exist as 'turn' like rather than '3_{10}-helix' structures (Fig. 4). It is well known that the

proline residue is a helix breaker since its highly strained backbone nitrogen is a part of a five membered ring. However, here the proline residue involves its CO group in hydrogen bonding, but not its backbone nitrogen atom. The two (alpha and beta) conformations of the proline cause this secondary structural change [115]. Also, the proline residue is located in a surface loop of 15 residues long, which thus may have more conformational flexibility. The conformation that results in a '3_{10}-helix' seems to be stabilized by the hydrogen bonds that result because of the Thr^{436} residue which is lacking in 4D due to the presence of Asn^{362} (4D numbering).

In all 4B '3_{10}-helix' structures the former trend was observed while the four 4B structures that contain a 'turn', have an orientation of the proline and hydrogen bonds similar to the 4D ('turn') structure. Though sequence differences can explain the secondary structure change between 4B and 4D, it cannot be implied for all 4B structures. The structural variation between '3_{10}-helix' and 'turn' in the M-loop region within PDE4B structures cannot be accounted for even with similar ligands and the same space group (Table **2**). After an extensive search, the only difference that we could find between these two sets of structures was the pH maintained during crystallization [69]. All '3_{10}-helix' containing structures were crystallized at pH-10.0 using polar solvents like $LiSO_4$ and NH_4SO_4 solution. In contrast all the 'turn' containing structures were crystallized in the pH range of 6.5-7.5 using polyethylene glycol (PEG). An electronic structure calculation on the model SPMCD residue sequence of PDE4 was performed to explain the thermodynamic preferences for the 'turn' secondary structure in the M-loop region [69]. This study reports that in the 'turn' and '3_{10}-helix' structures, protonation and deprotonation of the cysteine side chain and backbone amide bonds alter the non-covalent interactions established with adjacent residues (proline with aspartic acid and serine with cysteine) and solvent molecules (water or polyethylene glycol molecules) [69]. The secondary structures have similar sequences and hence may not account for the subtype selectivity of PDE4. Because a change in structure can originate due to pH variation from physiological pH (7.4-7.6), PDE4 could have a 'turn'-like secondary structure that would only be significantly different if the cellular pH were really altered in the distribution of 4B and 4D subtypes. Although the Thr^{436}/Asn^{362} pair does not seem to be decisive in the secondary structure alteration, it appears to be crucial to draw the differences between 4B and 4D. We investigated how this Thr^{436}/Asn^{362} mutation in the M-loop sequence helps to change the interactions with the inhibitor in the active site to bring out subtype selectivity.

3.3.1.2.2. Root Mean Square Deviation

To account for the differences existing between the 4B and 4D subtypes at the residue level, structures with similar ligands are structurally aligned using homology module of molecular operating environment (MOE) [116]. The following equation was applied to aligned structures to calculate residue-by-residue RMSD for the backbone [117].

$$RMSD = \sqrt{\frac{\sum_{i=1}^{N} d_i^2}{N}}$$

Where d_i is the distance between the i^{th} atoms and N is the number of such distances.

There are two structures each for 4B and 4D with cAMP, three each with rolipram and one each with cilomilast, piclamilast, roflumilast and pyrazole analogs (Table **2**). Superimposition of these structures and residue-by-residue backbone RMSD calculations have shown a deviation in the three loop regions in 4B and 4D structures, and the residues belonging to the loop regions showing the largest deviations are Glu^{317} and Glu^{318} (helix 10/11), Ser^{368} and Ser^{369} (loop between 12/13), and Pro^{430} and Met^{431} (M-loop). These results are comparable with the Cα-superimposition of 4B and 4D. The alterations in the backbone may also be responsible for variations in the active site. Hence, 32 active site residues that were reported earlier [110] and Pro^{430} were superimposed for 4B and 4D proteins with similar ligands and RMSD values were calculated for the side chains.

The cAMP containing structures show variations at Asp^{392} (~1.1 Å) and Asn^{395} (~1.4 Å). The two residues, Pro^{430} (1.6 Å – 3.7 Å) and Ser^{429} (1.4 Å – 1.6 Å) show strong deviations from 4D and the variation is greater for '3_{10}-helix' containing 4Bs (~3.7 Å) than 'turn' containing 4Bs (~1.6 Å). Met^{431} (located in the M-loop region), an important hydrophobic residue of the Q2 pocket of the active site, shows a deviation ranging from 1.7 Å – 2.6 Å. Probably, the absence of a hydrophobic group in cAMP might allow greater flexibility to the Met residue (Fig. **5a**). Apart from the abovementioned residues, very slight alterations (>0.4 Å) have been noticed for Met^{347}, Trp^{406}, Ile^{410}, Met^{411}, Glu^{413}, Cys^{432}, Val^{439} and Ser^{442} in all cAMP structures. Also, the important role of a few residues such as Trp^{406} in the catalytic activity has been shown by site directed mutagenesis studies [81].

When it comes to rolipram, the two residues that deviate in the cAMP-containing structures, Asp^{392} and Asn^{395}, also show variations of 1.1 Å and 1.2 Å respectively. Comparatively, the Met^{431} residue was more strongly displaced in the cAMP-containing structures (1.75 Å - 2.58 Å) than in the rolipram-containing structures (0.40 Å – 0.91 Å) (Fig. **5a, b**). We can, therefore, deduce that as the cyclopentoxy group of rolipram is positioned in the Q2 pocket and show hydrophobic interactions with Met^{431} [49], hence the residue is not very flexible. Apart from the three residues, notable differences have been observed for Ser^{429} (1.44 Å – 1.59 Å) and Pro^{430} (1.4 Å – 3.6 Å). Finally, Cys^{432}, Val^{439} and Ser^{442}, which are in the M-loop region, show a slightly smaller variation. The Met^{411} residue located in the loop region of helix 11/12 is altered exclusively in 1XN0 (4B), and this residue has been reported to be altered in PDEs and in turn to affect the rolipram sensitivity [118].

Lastly, cilomilast, piclamilast, roflumilast and pyrazole-containing 4B's illustrate deviation from 4D at Asp^{392} and in the strip of the M-loop region (Ser^{429}-Cys^{432}) followed by Val^{439} and Ser^{442} (Fig. **5c**). In the case of the pyrazole (1Y2J), the Gln^{417} residue located in the solvent pocket is displaced, which may account for its ligand specific nature (Fig. **5c**). In order to highlight the differences between 4B and 4D an attempt was made to correlate a few mutated residues (Thr/Asn) with residues that have shown structural variations in the M-loop region.

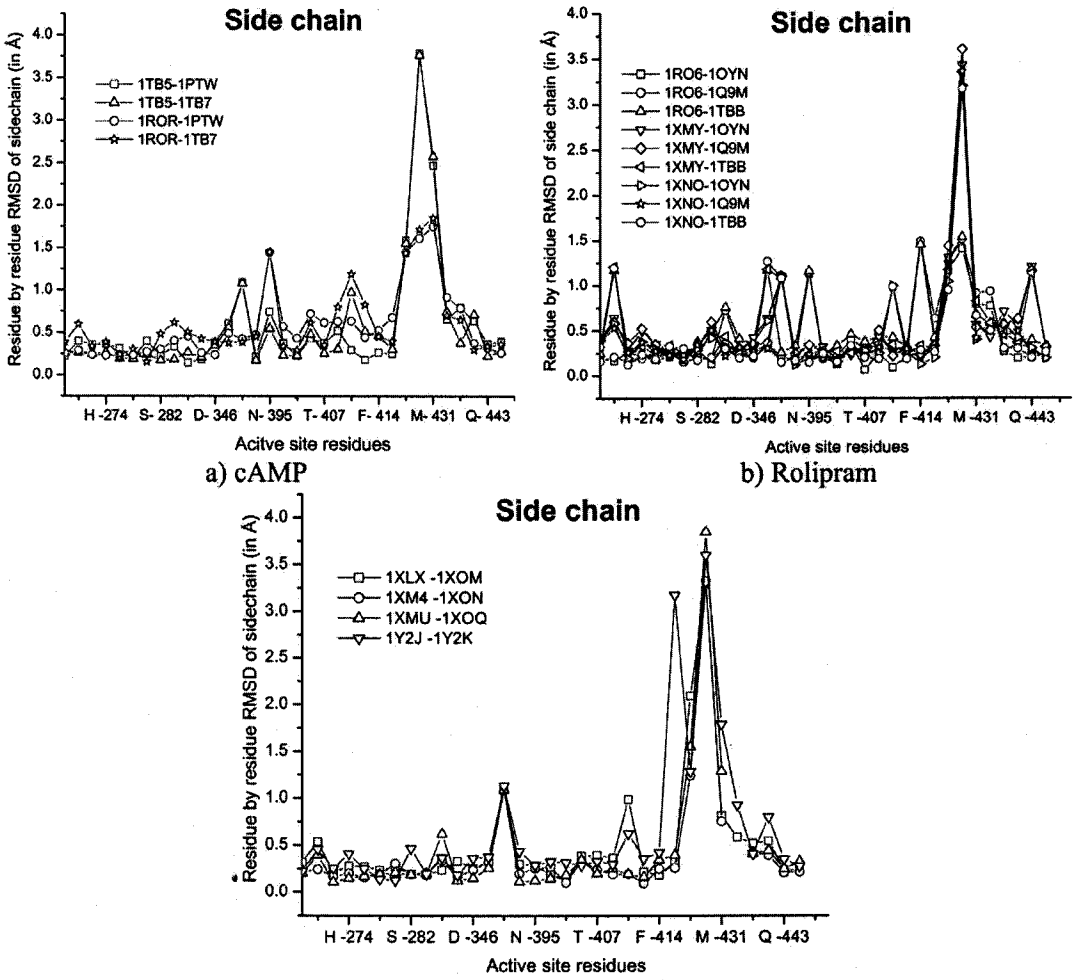

Fig. (5). Comparison of RMSD values for active site residues of both 4B and 4D structures that have similar ligands, plotted in panels **a, b** and **c**.

3.3.2. Impact of the M-Loop Region on Inhibitor Selectivity

RMSD values and hydrogen bonding patterns have clearly established the variations in the M-loop region of 4B and 4D. The previous studies have also suggested that there is a decisive role of the M-loop region in determining inhibitor selectivity towards PDE4 [58, 59]. Accordingly, we ventured to decipher the molecular properties that would bring out the differences between both subtypes and subsequently provide some structural clues to explain the selectivity.

3.3.2.1. Hydrophobicity

In general, hydrophobic residues tend to be more buried in the interior of the molecule and hydrophilic residues are more exposed to the solvent and therefore, a profile of these values can specify the overall folding pattern. The values also provide the general trend of hydropathic values in a sequence.

Genchek [119a] was used to calculate the hydrophobicity values. The hydrophobicity scale derived by Kyte and Doolittle was implemented in the present analysis [119b]. The moving window averages of 7, 9, 11 and 13 and default hydrophobic scaling were considered as a smoothing function in Genchek. The hydrophobic maps were generated using the MOLCAD surface of Sybyl 6.9 wherein Crippen lipophilic values were implemented to compute the hydrophobicity [120, 121].

The computed hydrophobic values for 4B and 4D showed significant differences in the M-loop region where the Thr/Asn mutation was noticed (Fig. **6**). Because of the presence of the Thr^{436} (HP- 0.72) residue, the hydrophobic nature of Lys^{434} (–4.16 for 4B, –6.44 for 4D) and His^{435} (–1.56 for 4B, –3.16 for 4D) is greater than in 4D where Asn^{359} (–0.48) replaces the threonine residue and makes the loop region less hydrophobic. A single mutation, rarely, or multiple mutations, most often, affect the property of a nearby residue, which is five or more than five residues away and in turn the substrate selectivity seen in the cGMP specific PDEs can be ascribed to the Glu residue [79]. Similarly, in the present study the Thr^{436}/Asn^{359} residues, which are located at the fifth position from Met^{431}, decrease the hydrophilicity of Met^{431} and in turn its interactions with the ligand.

The HP values, which are quantified with varying window sizes (13, 11, 9 and 7), show the stronger hydrophilic nature of the 4D residues. With window size 13, where the

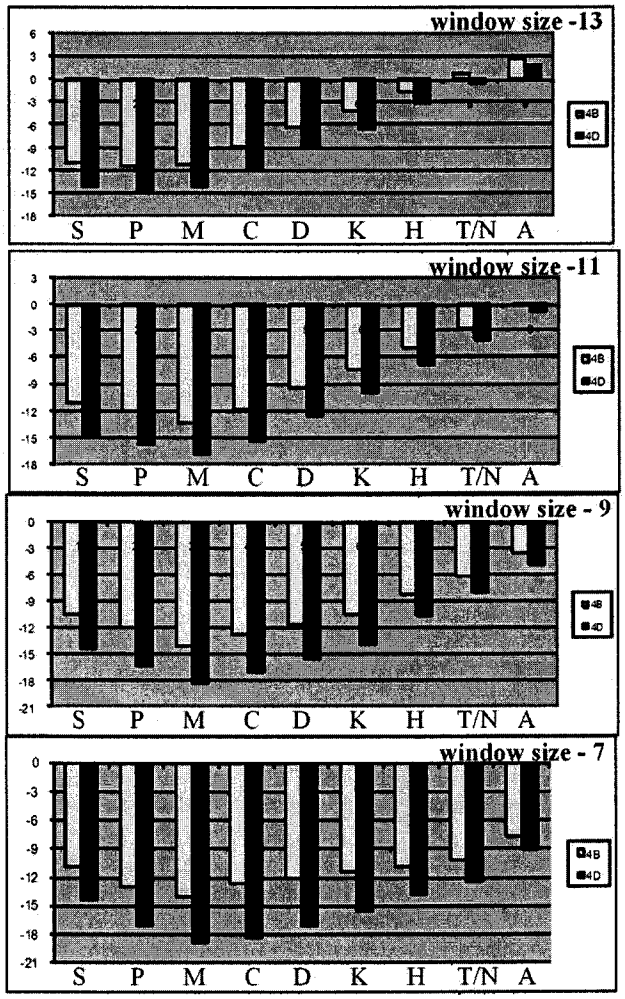

Fig. (6). Varied window sizes of 13, 11, 9 and 7 are considered for hydrophobicity values of nine important residues that are present in the M-loop region of 4B and 4D. The plots are generated for the numbers that are in bold in the table and are obtained from the program Genchek where abscissa represents the amino acid numbers and ordinate indicates the relative hydrophobicity. The values above the axis denote hydrophobic regions and the values below the axis refer to hydrophilic regions. The table pertains to hydrophobic values at window size 13 of all-important residues of M-loop. The fasta formats that are used for both 4B and 4D are taken from the PDB.

mean of 13 residues will be plotted at the 7th residue, the change in hydropathic values from hydrophobic to hydrophilic can be traced for the Thr/Asn mutated residue and its impact is shown on the Met^{431} residue (Fig. **6**). Irrespective of the window size, Met^{431} is less hydrophilic in 4B (−11.17) with respect to 4D (−14.25). This variation is not only restricted to the methionine residue but other residues including Ser^{429} to Ala^{437} are also less hydrophilic in 4B than 4D. Similarly, Asp^{419} to Arg^{422} residues are more hydrophobic in 4B than 4D in that particular region (Fig. **6**). The inference that one can draw from the above results is the presence of considerable variation in the hydrophobic values of the 4B and 4D residues in the M-loop region.

Finally, the MOLCAD surface of the M-loop residues portrayed according to their hydrophobicity also shown that 4B is more hydrophobic (brown and green colors in Fig. **7a**) and 4D is more hydrophilic (blue color in Fig. **7a**). These variations may also be reflected in the protein-ligand interactions and in turn in the inhibitory activity. Interestingly, it does not seem that any inhibitor described until now has make use of this region effectively [26]. Therefore, the groups with greater hydrophobicity could achieve considerable selectivity for 4B over 4D [58].

3.3.2.2. MOLCAD Surface

In order to ensure the possibility of exploiting the M-loop, the size of the pocket was estimated by calculating the MOLCAD surfaces and various physico-chemical properties were mapped on these surfaces and color-coded. Moreover, to understand the selectivity and specificity of enzymatic reactions it is useful to have information about the flexibility of certain surface parts based on the temperature factor. The total available binding space, topology and nature of the pocket were estimated from fast Connolly channels for both 4B and 4D with different ligands.

The Sybyl 6.9 suite of program was used to calculate the MOLCAD surfaces for the M-loop region of 4B and 4D. The monomers of downloaded proteins were considered after removing water and other small molecules. After adding hydrogens, dummy atoms were defined from the residues

surrounding the entrance of the M-loop. The surfaces were generated according to fast Connolly and fast Connolly channel where the surface between the CPK model of the molecule and a probe sphere of 1.4 Å radius was considered [120]. The flexibility of the cavity was measured based on the temperature factor (B-factor) of each atom of a residue that was taken from the PDB coordinates. The 4B structure crystallized with cAMP (1TB5-698.22) differed slightly from 4D (1PTW- 696.18). 4D structures crystallized with rolipram analogs such as rolipram, cilomilast, piclamilast and R-mesopram have considerably larger areas compared to 4B (Table 3). The topology of the active site reveals that two channels, one in the M-loop and the other between helices 14 and 8, open towards the solvent region for both 4B and 4D. Interestingly, the M-loop channel was not observed in the cAMP-containing PDE4s but noticed in the rolipram-containing analogues (Figs. **7b** and **c**). Hence, we infer that the entrance to the M-loop region (channel), which is lined by Met^{411}, Phe^{414}, Met^{431}, Ala^{437}, Ser^{438} and Ser^{442}, opens after the binding of rolipram analogues but not with cAMP, as it does not have any suitable group to interact with the residues in this region.

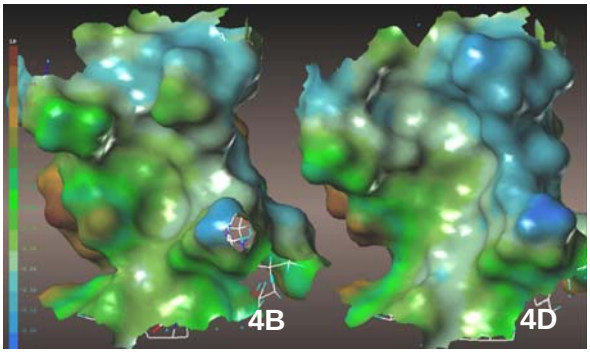

A

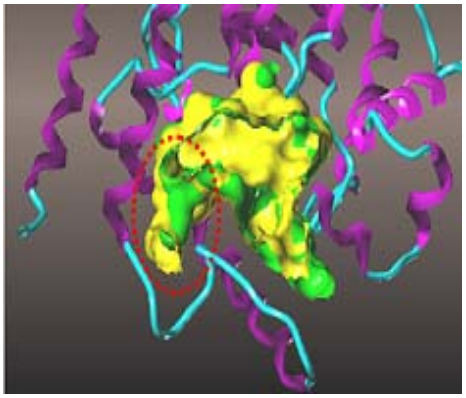

B

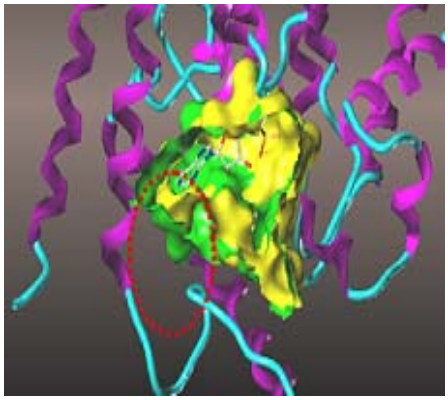

C

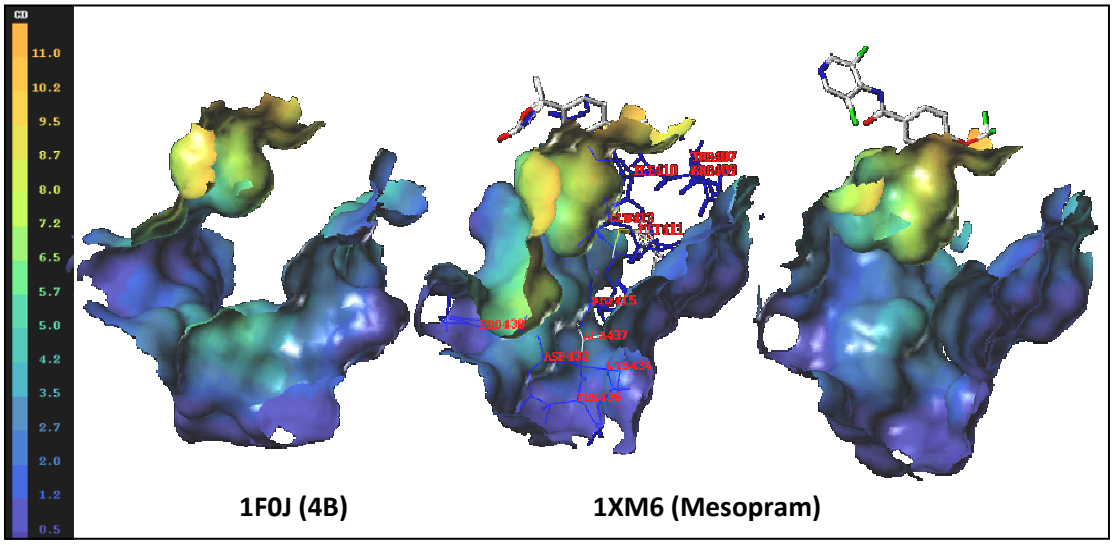

D

Fig. (7A). The MOLCAD surface is generated for the M-loop region using Sybyl. The surface is colored by lipophilicity where brown to blue represents hydrophobic to hydrophilic. 4B is hydrophobic in nature compared to 4D where the threonine residue is mutated to asparagine in 4D and changes the property to hydrophilic. **B** & **C**) Fast Connolly channel that is generated for both 4B (green) and 4D (yellow) having a) cilomilast b) cAMP ligands. The channel that is located in the M-loop is highlighted in red dotted ellipses. Protein tertiary structure is displayed in magenta helices and cyan loops while the ligand is shown in capped stick rendering. **D**) Comparing the cavity depth of M-loop region for 4B without ligand (1F0J), with mesopram (1XM6) and roflumilast (1XMU) by means of MOLCAD surfaces. The color is coded according to the cavity depth wherein blue to yellow represents accessible to buried surface. For clarity of the picture, important residues are shown only for 1XM6 in atom wire frame and ligands are displayed as capped stick models.

The M-loop was further analyzed in detail by taking a 10 Å radius from a dummy atom that was created from residues Met[411], Met[431], Ala[437] and Val[439] (Fig. **8**). The residues Met[431] and Ala[437] were involved in dummy atom generation since

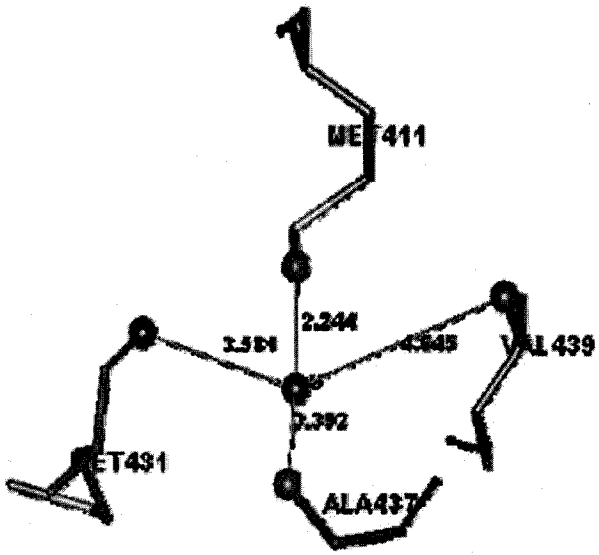

Fig. (8). The four residues that are considered to define the dummy atom. The atoms that are involved are displayed as ball models and approximate distances (in Å) from the dummy atom are shown in lines. However, these distances vary slightly with each protein.

the hydrophobicity values were notably different for these two besides showing deviation in their conformations (RMSD and hydrogen bond interactions). Also, they are located at the mouth of the M-loop where they can possibly show differences between 4B and 4D. The 10 Å region includes the following residues: Met[411], Phe[415], Pro[430], Met[431], Cys[432], Asp[433], Lys[434], His[435], Thr[436], Ala[437], Ser[438], Val[439] and Ser[442]. A comparison of the protein with no ligand (1F0J), with ligand-containing structures had shown a significant change in the volume as well as the area for these proteins (Fig. **7d**). The results show that 4B ligands occupy smaller areas compared to 4D ligands with an exception of rolipram. For instance, various 4B and 4D ligands have the following areas: rolipram 855.26, 919.62 (1XMY, 1XN0), and 844.16, 838.49 for 4D (1OYN, 1TBB), roflumilast 821.87 (1XMU) and 858.64 (1XOQ), cilomilast 821.75 (1XLX) and 866.99 (1XOM), and piclamilast 812.05 (1XM4) and 860.29 (1XON), respectively (Table **3**). The dissimilarity might arise from the Met[431] side chain conformation. The comparison of 4B mesopram (858.59) and 4B without ligand (1F0J- 907.87) suggests that the *n*-propyl chain of mesopram (1XM6) has very effective access to the region, which was buried in 1F0J (Fig. **7d**). Thus, we infer from the above observation that the buried area of the ligand-free protein (1F0J) becomes accessible when the ligand binds, and the percentage of accessibility varies with type of the ligand. Comparatively, the PDE4s that are crystallized with cAMP have lower accessible areas (4B-792.60 and 4D-803.73) since they do not have a suitable group to penetrate this region. Therefore, in designing subtype selective ligands, considering the M-loop region seems to be more important when compared to the preserved space that is available on either side of metal ions (Fig. **7b** and **c**).

Table 3. MOLCAD Surface Volumes (in Å^3) of Active Site and M-Loop Regions for Both PDE4B and 4D Structures with Various Ligands

Ligand	PDE4		MOLCAD Surface Volume	
	Type	PDBID	Active Site	M-Loop
cAMP	4B	1TB5	698.22	792.60
	4D	1PTW	696.18	803.73
Rolipram	4B	1XMY	870.55	855.26
		1XN0	809.87	919.62
	4D	1OYN	913.80	844.16
		1TBB	940.89	838.49
Cilomilast	4B	1XLX	760.97	821.75
	4D	1XOM	789.76	866.99
Roflumilast	4B	1XMU	731.80	821.87
	4D	1XOQ	783.85	858.64
Piclamilast	4B	1XM4	744.38	812.05
	4D	1XON	762.87	860.29
Mesopram	4B	1XM6	769.06	858.59
No ligand	4B	1F0J	-	907.87

4. DESIGNING NEW DRUG CANDIDATES

The catalytic pockets of PDE4B and 4D have significant subtle differences and by careful manipulation of the chemical structure of inhibitors it should be possible to design new drug candidates with improved subtype selectivity. The docking and co-crystal structural analyses suggest that the ideal PDE4 inhibitor should have a) an aromatic motif to have stacking and hydrophobic interactions with Phe, Ile and Met residues; b) hydrogen bond acceptors to interact with Gln^{443}; c) A hydrophobic group on the aromatic ring that can be accommodated in the Q1 and Q2 pockets (lining of M-loop); d) a polar tail group that will have electrostatic interactions with the metal atoms; e) an aromatic ring with a polar group could also have interactions with the solvent pocket which is rich in histidine residues (Fig. **9**). An extensive virtual screening of drug databases with these characteristics can open a new dimension for initial guesses about the next generation of PDE4 inhibitors with enhanced activity. However, subtype selective drugs may have complex mechanisms, which can be revealed only by solving the full-length protein.

5. CONCLUSIONS

The present review comprehensively addresses the issue of therapeutic development of PDE4 analogs and proposes that subtype selectivity is one of the most important parameters, where a consensus is rapidly emerging. The advantages and disadvantages of five strategies to minimize the side effects of PDE4 inhibitors such as selectivity towards high affinity vs. low affinity form, low BBB permeability, inhaled drugs, dual specific PDE's and subtype selectivity, are reviewed. In the midst of these strategies subtype selectivity has its own advantage in the design of anti-inflammatory agents due to differential tissue distribution. Among the four subtypes, gene knockout studies and biochemical studies support PDE4B2 as an ideal target. However, achieving subtype selectivity is a bottleneck for rational drug design due to high conservation of the active site residues of the catalytic domain in the subtypes. The finer differences found in the three dozen available crystal structures of PDE4B and 4D show that a backbone deviation of Pro^{430} and in turn its tendency to form hydrogen bonds with Asp^{433} result in the secondary structure alteration of 3_{10}-helix versus turn in the M-loop region. This change is determined by the pH of crystallization conditions that alter protonation and deprotonation of cysteine and amide bonds which in turn alter non-covalent interactions with the adjacent residues and solvent molecules of the SPMCD residues of the M-loop region. A single mutation of the Thr^{436}/Asn^{362} pair in the M-loop changes the hydrogen bonding patterns and hydrophobicity between 4B and 4D subtypes. Lastly, an impact of the M-loop is observed from hydrophobicity and MOLCAD surfaces which have shown 4B to be more hydrophobic than 4D. Various crystal structures and docking studies have explained that an ideal PDE4 inhibitor should have an aromatic motif to have hy-

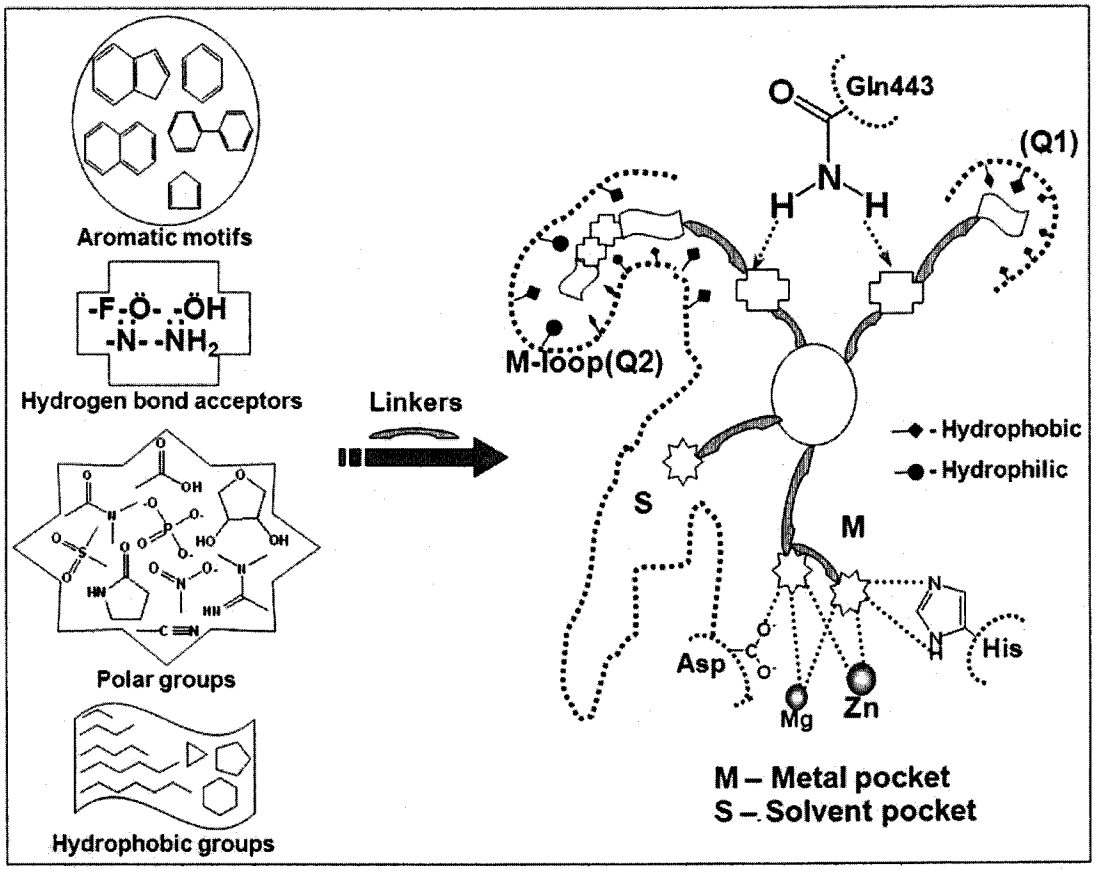

Fig. (9). Schematic representation of the four different types of fragments connected through linkers, which outlines the basic idea for the design of new drug candidates through virtual screening.

drophobic interactions with Phe, Ile and Met, and that a polar tail group to interact with a metal or solvent binding pocket in the active site enhances the potency. Thus far, inhibitors have been developed with access to the metal and solvent pocket. We assume that attention to the hydrophobic pocket can lead to effective probes of subtype selectivity.

ACKNOWLEDGEMENTS

PS and DU thank CSIR, New Delhi for the award of senior research fellowships. DBT, New Delhi is thanked for providing the financial support to carry out the work.

REFERENCES

[1] a) Sutherland EW, Rall TW. Fractionation and characterization of a cyclic adenine ribonucleotide formed by tissue particles. J Biol Chem 1958; 232: 1077-1091. b) Jonathan B, Sucha S, Subha S. Profiling human phosphodiesterase genes and splice isoforms. Biochem Biophys Res Comm 2006; 350: 25-32.

[2] Beavo JA, Hardman G, Sutherland EW. Hydrolysis of cyclic guanosine and adenosine 3',5'-monophosphates by rat and bovine tissues. J Biol Chem 1970; 245: 5649-55.

[3] Beavo JA. Cyclic nucleotide phosphodiesterases: Functional implications of multiple isoforms. Physiol Rev 1995; 75: 725-48.

[4] Bender AT. Baevo AJ. Cyclic nucleotide phosphodiesterases: Molecular regulation to clinical use. Pharmacol Rev 2006; 58: 488-520.

[5] Sharron HF, Illarion VT, Jackie DC. Cyclic nucleotide phosphodiesterases: relating structure and function. Prog Nucleic Acid Res Mol Biol 2001; 65: 1-52.

[6] Soderling SH, Beavo JA. Regulation of cAMP and cGMP signaling: New phosphodiesterases and new functions. Curr Opin Cell Biol 2000; 12: 174-79.

[7] Menniti FS, Faraci WS, Christopher SJ. Phosphodiesterases in the CNS: Targets for drug development. Nat Rev Drug Discov 2006; 5: 660-70.

[8] Teixeira MM, Gristwood RW, Cooper N, Hellewell PG. Phosphodiesterase (PDE4) inhibitors: Anti-inflammatory drugs of the future? Trends Pharmacol Sci 1997; 18: 164-71.

[9] Spina D, Landells LJ, Page CP. The role of phosphodiesterase enzymes in allergy and asthma. Adv Pharmacol 1998; 44: 33-89.

[10] Zheng H, Mancini JA. Phosphodiesterase 4 inhibitors for the treatment of asthma and COPD. Curr Med Chem 2006; 13: 3253-3262.

[11] Trophy TJ. Phosphodiesterase isozymes molecular targets for novel antiasthmatic agents. Am J Respir Crit Care Med 1998; 157: 351-70.

[12] Castro A, Jerez MJ, Martinez A, Gil C. Cyclic nucleotide phosphodiesterases and their role in immunomodulatory responses: Advances in the development of specific phosphodiesterase inhibitors. Med Res Rev 2005; 25: 229-44.

[13] Bolger G, Michaeli T, Martins T, St John T, Steiner B, Rodgers L, *et al.* A family of human phosphodiesterases homologous to the dunce learning and memory gene product of Drosophila melanogaster is potential targets for antidepressant drugs. Mol Cell Biol 1993; 13: 6558-71.

[14] Houslay MD. PDE4-cAMP-specific phosphodiesterases. Prog Nucleic Acid Res Mol Biol 2001; 69: 249-315.

[15] Dastidar SG, Rajagopal D, Ray A. Therapeutic benefit of PDE4 inhibitors in inflammatory diseases. Curr Opin Invest Drugs 2007; 8: 364-72.

[16] Bolger GB, Erdogan S, Jones RE, Loughney K, Scotland G, Hoffmann R, *et al.* Characterization of five different proteins produced by alternatively spliced mRNAs from the human cAMP-specific phosphodiesterase PDE4D gene. Biochem J 1997; 328: 539-48.

[17] Houslay MD, Sullivan M, Bolger GB. The multienzyme PDE4 cyclic adenosine monophosphate-specific phosphodiesterase family: Intracellular targeting, regulation, and selective inhibition by compounds exerting anti-inflammatory and antidepressant actions. Adv Pharmacol 1998; 44: 225-342.

[18] Houslay DM, Adams RD. PDE4 cAMP phosphodiesterases: Modular enzymes that orchestrate signaling cross talk, desensitization and compartmentalization. Biochem J 2003; 370: 1-18.

[19] Muller T, Engels P, Fozard JR. Subtypes of the type4 cAMP phosphodiesterase: Structure, regulation and selective inhibition. Trends Pharmacol Sci 1996; 17: 294-98.

[20] a) Spina D. Phosphodiesterase-4 inhibitors in the treatment of inflammatory lung disease. Drugs 2003; 63: 1-20. b) Boswell-Smith V, Spina D, Page CP. Phosphodiesterase inhibitors. Br J Pharmacol 2006; 147: S252-7.

[21] Zheng H, Joseph AM. Phosphodiesterase 4 inhibitors for the treatment of asthma and COPD. Curr Med Chem 2006; 13: 3253-62.

[22] Jeffery P. Phosphodiesterase-4 selective inhibition: Novel therapy for the inflammation of COPD. Pul Pharm Ther 2005; 18: 9-17.

[23] Barnes PJ. Theophylline: New perspective for the old drug. Am J Respir Crit Care Med 2003; 167: 813-818.

[24] Boswell-Smith V, Cazzola M, Page CP. Are phosphodiesterase 4 inhibitors just more theophylline? J Allergy Clin Immunol 2006; 117: 1237-43.

[25] Piaz DV, Giovannoni MP. Phosphodiesterase 4 inhibitors, structurally unrelated to rolipram, as promising agents for the treatment of asthma and other pathologies. Eur J Med Chem 2000; 35: 463-480.

[26] Burnouf C, Pruniaux MP. Recent advances in PDE4 inhibitors as immunoregulators and anti-inflammatory drugs. Curr Pharm Des 2002; 8: 1255-1296.

[27] Montana JG, Dyke HJ. Phosphodiesterase 4 inhibitors. Ann Rep Med Chem 2001, 36: 41-56.

[28] Spina D. The potential of PDE4 inhibitors in respiratory disease. Curr Drug Target Inflamm Allergy 2004; 3: 231-46.

[29] Giembycz MA. Development status of second generation PDE4 inhibitors for asthma and COPD: The story so far. Monaldi arch Chest Dis 2002; 57: 48-64.

[30] Zhang KY, Ibrahim PN, Gillette S, Bollag G. Phosphodiesterase 4 as a potential drug target. Exp Opin Ther drugs 2005; 9: 1283-04.

[31] Trophy TJ, Page C. Phosphodiesterases: The journey towards therapeutics. Trends Pharmacol Sci 2000; 21: 158-9.

[32] Lipworth BJ. Phosphodiesterase-4 inhibitors for asthma and chronic obstructive pulmonary disease. Lancet 2005; 365: 167-75.

[33] Huang Z, Ducharme Y, Macdonald D, Robichaud A. Next generation of PDE4 inhibitors. Curr Opin Cell Biol 2001; 5: 432-38.

[34] Beavo JA, Francis SH, Houslay MD. Medicinal chemistry of PDE4 inhibitors. Cyclic Nucleotide Phosphodiest Health Dis 2007; 667-99.

[35] Souness JE, Rao S. Proposal for pharmacologically distinct conformers of PDE4 cyclic AMP phosphodiesterases. Cell Signal 1997; 9: 227-36.

[36] Barnette MS, Bartus JO, Burman M, Christensen SB, Cielslinski LB, Esser KM, *et al.* Association of the anti-inflammatory activity of phosphodiesterase 4 (PDE4) inhibitors with either inhibition of PDE4 catalytic activity or competition for [3H] rolipram binding. Biochem Pharmacol 1996; 51: 949-56.

[37] Duplantier AJ, Biggers MS, Chambers RJ, Cheng JB, Cooper K, Damon DB, *et al.* Biarylcarboxylic acids and -amides: Inhibition of phosphodiesterase type IV versus [3H] rolipram binding activity and their relationship to emetic behavior in the ferret. J Med Chem 1996; 39: 120-5.

[38] Zhang HT, Zhao Y, Huang Y, Deng C, Hopper AT, Vivo MD, *et al.* Antidepressant-like effects of PDE4 inhibitors mediated by the high-affinity rolipram binding state (HARBS) of the phosphodiesterase-4 enzyme (PDE4) in rats. Psychopharmacology 2006; 186: 209-17.

[39] Lamontagne S, Meadows E, Luk P, Normandin D, Muise E, Boulet L, *et al.* Localization of phosphodiesterase-4 isoforms in the medulla and nodose ganglion of the squirrel monkey. Brain Res 2001; 920: 84-96.

[40] Houslay MD, Schafer P, Zhang KYJ. Phosphodiesterase-4 as therapeutic target. Drug Discov Today 2005; 10: 1503-19.

[41] Giembycz MA. 4D or not 4D the emetogenic basis of PDE4 inhibitors uncovered? Trends Pharmacol Sci 2002; 23: 548.

[42] Manning CD, Burman M, Christensen SB, Cieslinski LB, Essayan DM, Grous M, *et al.* Suppression of human inflammatory cell function by subtype-selective PDE4 inhibitors correlates with inhibition of PDE4A and PDE4B. Br J Pharmacol 1999; 128: 1393-8.

[43] Jin S-LC, Richter W, Conti M. Insights into the physiological functions of PDE4 from knockout mice. Cyclic Nucleotide Phosphodiest Health Dis 2007; 323-46

[44] Hansen G, Jin S-LC, Umetsu DT, Conti M. Absence of muscarinic cholinergic airway responses in mice deficient in the cyclic nucleotide phosphodiesterase PDE4D. Proc Nat Acad Sci USA 2000; 97: 6751-6.

[45] Jin S-LC. Conti M. Induction of the cyclic nucleotide phosphodiesterase PDE4B is essential for LPS-activated TNF-α response. Proc Nat Acad Sci USA 2002; 99: 7628-33.

[46] Robichaud A, Stamatiou PB, Jin SL, Lachance N, MacDonald D, Laliberte F, *et al.* Deletion of phosphodiesterase 4D in mice shortens α(2)-adrenoceptor-mediated anesthesia, a behavioral correlate of emesis. J Clin Invest 2002; 110: 1045-52.

[47] Hughes B, Owens R, Perry M, Warrellow G, Allen R. PDE4 inhibitors: The use of molecular cloning in the design and development of novel drugs. Drug Discov Today 1997; 2: 89-101.

[48] Barber R, Baillie GS, Bergmann R, Shepherd MC, Sepper R, Houslay MD, *et al.* Differential expressions of PDE4 cAMP phosphodiesterase isoforms in inflammatory cells of smokers with COPD, smokers without COPD, and nonsmokers. Am J Physiol Lung Cell Mol Physiol 2004; 287: L332-43.

[49] Wang P, Wu P, Ohleth KM, Egan RW, Billah MM. Phosphodiesterase 4B2 is the predominant phosphodiesterase species and undergoes differential regulation of gene expression in human monocytes and neutrophils. Mol Pharmacol 1999; 56: 170-4.

[50] Chung KF. Phosphodiesterase inhibitors in airways disease. Eur J Pharm 2006; 533: 110-7.

[51] a) Deng Y, Qiang-min X, Hui-fang T, Jian-gang S, Jun-fang D, Jiqiang C, *et al.* Effects of ciclamilast, a new PDE4 inhibitor, on airway hyperresponsiveness, PDE4D expression and airway inflammation in a murine model of asthma. Eur J Pharm 2006; 547: 125-35. b) Kroegel C, Foerster M. Phosphodiesterase-4 inhibitors as a novel approach for the treatment of respiratory disease: cilomilast. Exp Opin Investigational drugs 2007; 16: 109-24.

[52] Hersperger R, Bray –French K, Mazzoni L, Müller T. Palladium catalyzed cross-coupling reactions for the synthesis of 6,8-Disubstiuted 1,7-Naphthyridines: A novel class of potent and selective Phosphodiesterase type 4D inhibitors. J Med Chem 2000, 43, 675-682. b) Hersperger R, Dawson J, Müller T. Synthesis of 4-(8-benzo[1,2,5]oxadiazol-5-yl-[1,7]naphthyridine-6-yl)-benzoic acid: a potent and selective phosphodiesterase type 4D inhibitor. Bioorg Med Chem Lett 2002; 12: 233-5.

[53] Huang Z, Dias R, Jones T, Liu S, Styhler A, Claveau D, *et al.* L-454,560, a potent and selective PDE4 inhibitor with *in vivo* efficacy in animal models of asthma and cognition. Biochemical Pharmacology 2007; 73: 1971-81.

[54] Lin J, Pahlke G, Conti M. Activation of the cAMP-specific phosphodiesterase PDE4D3 by phosphorylation. J Biol Chem 1999; 274: 19677-85.

[55] Huang Z, Liu S, Zhang L, Salem M, Greig GM, Chan CC, *et al.* Preferential inhibition of phophodiesterase 4 by ibudilast. Life Sciences 2006; 78: 266-8.

[56] Giovannoni MP, Cesari N, Graziano, A, Claudia V, Claudio B, Biagini Pierfrancesco B, *et al.* Synthesis of pyrrolo[2,3-d]pyridazinones as potent, subtype selective PDE4 inhibitors. J Enzyme Inhib and Med Chem 2007; 22: 309-18.

[57] Xu RX, Rocque WJ, Lambert MH, Vanderwall DE, Luther MA, Nolte RT. Crystal structures of the catalytic domain of phosphodiesterase 4B complexed with AMP, 8-Br-AMP, and rolipram. J Mol Biol 2004; 337: 355-65.

[58] Huai Q, Wang H, Sun Y, Kim HY, Liu Y, Ke H. Three-dimensional structures of PDE4D in complex with roliprams and implication on inhibitor selectivity. Structure 2003; 11: 865-73.

[59] Huai Q, Liu Y, Francis SH, Corbin JD, Ke H. Crystal structures of phosphodiesterases 4 and 5 in complex with inhibitor 3-isobutyl-1-methylxanthine suggest a conformation determinant of inhibitor selectivity. J Biol Chem 2004; 279: 13095-101.

[60] Charpiot B, Bitsch F, Buchheit KH, Channez P, Mazzoni L, Muller T, *et al.* Disease activated drugs: A new concept for the treatment of asthma. Bioorg Med Chem 2001; 9: 1793-805.

[61] Morphy R, Rankovic Z. Designed multiple ligands. An emerging drug discovery paradigm. J Med Chem 2005; 48: 6523-43.

[62] Giembycz MA. Life after PDE4: Overcoming adverse events with dual-specificity phosphodiesterase inhibitors. Curr Opin in Pharm 2005; 5: 238-44.

[63] Jones NA, Leport M, Holand T, Vos T, Morgan M, Fink M, *et al.* Phosphodiesterase (PDE) 7 in inflammatory cells from patients with asthma and COPD. Pul Pharma Therap 2007; 20: 60-8.

[64] Giembycz MA, Smith SJ. Phosphodiesterase 7A: a new therapeutic target for alleviating chronic inflammation? Curr Pharm Des 2006; 12: 3207-20.

[65] Sasaki T, Kotera J, Yuasa K, Omori K. Identification of human PDE7B, a cAMP-specific phosphodiesterase. Biochem Biophys Res Commun 2000; 271: 575-83.

[66] Barnette MS, Giembycz MA, Smith SJ, Fazakerley SB. Donnelly LE. Barnes PJ. Ubiquitous expression of phosphodiesterase 7A in human proinflammatory and immune cells. Am J Physiol Lung Cell Mol Physiol 2006; 284: 279-89.

[67] Smith SJ, Cieslinski LB, Newton R, Donnelly LE, Fenwick PS, Nicholson AG, *et al.* Discovery of BRL 50481 [3-(N,N-dimethylsulfonamido)-4-methyl-nitrobenzene], a selective inhibitor of phosphodiesterase 7: *In vitro* studies in human monocytes, lung macrophages, and CD8 T-lymphocytes. Mol Pharmacol 2004; 66: 1679-89.

[68] Yamamoto S, Sugahara S, Naito R, Ichikawa A, Iked K, Yamada T, *et al.* The effects of a novel phosphodiesterase 7A and -4 dual inhibitor, YM-393059, on T-cell-related cytokine production *in vitro* and *in vivo*. Eur J Pharm 2006; 541: 106-14.

[69] Usharani D, Srivani P, Sastry GN, Jemmis ED. A pH dependence of 3_{10}-helix versus turn in m-loop region of PDE4: Observations on PDB entries and an electronic structure study. J Chem Theor Comp 2008; 4: 974-84.

[70] Salter EA, Wierzbicki A. The mechanism of cyclic nucleotide hydrolysis in the phosphodiesterase catalytic site. J Phys Chem B 2007; 111: 4547-52.

[71] Salter EA, O'Brien KA, Edmunds RW, Wierzbicki A. ONIOM investigation of nucleotide selectivity in phosphodiesterases 3 and 4. Int J of Quant Chem 2008; 108: 1189-99.

[72] Xiong Y, Lu H-T, Li Y, Yang G_F, Zhan C-G. Characterization of a catalytic ligand bridging metal ions in PDE4 and 5 by molecular dynamics simulations and hybrid quantum mechanical/molecular mechanical calculations. Biophys J 2006; 91: 1858-67.

[73] Kang NS, Chae CH, Yoo S.-E. Study on the hydrolysis mechanism of phosphodiesterase 4 using molecular dynamics simulations. Mol Simulation 2006; 32: 369-74.

[74] a) Reddy AS, Priyadarshini PS, Kumar PP, Pradeep HN, Sastry GN. Virtual screening in drug discovery – A computational perspective. Current Protein and Peptide Science 2007; 8: 329-51. b) Krier M, de Araujo-Junior JX, Schmitt M, Duranton J, Basaran HJ, Lugnier C, *et al.* Design of small-sized libraries by combinatorial assembly of linkers and functional groups to a given scaffold: Application to the structure-based optimization of a phosphodiesterase4 inhibitor. J Med Chem 2005; 48: 3816-22.

[75] Polymeropoulos EE, Hofgen N. A peptidic binding site model for PDE4 Inhibitors. QSAR 1999; 18: 543-7.

[76] Richter W, Unciuleac L, Hermsdorf T, Kronbach T, Dettmer D. Identification of inhibitor binding of the cAMP-specific phosphodiesterase 4. Cell Signal 2001; 13: 287-97.

[77] Pillai R, Kytle K, Reyes A, Colicelli J. Use of a yeast expression system for the isolation and analysis of drug-resistant mutants of a mammalian phosphodiesterase. Proc Nat Acad Sci USA 1993; 90: 11970-4.

[78] Jacobitz S, Ryan MD, McLaughlin MM, Livi GP, DeWolf WE, Torphy TJ. Role of conserved histidines in catalytic activity and inhibitor binding of human recombinant phosphodiesterase 4A. Mol Pharmacol 1997; 51: 999-1006.

[79] Turko IV, Francis SH, Corbin JD. Hydropathic analysis and mutagenesis of the catalytic domain of the cGMP-binding cGMP-specific posphodiesterase (PDE5): cGMP versus cAMP substrate selectivity. Biochemistry 1998; 37: 4200-5.

[80] Atienza JM, Susanto D, Huang C, McCarty AS, Colicelli J. Identification of inhibitor specificity determinants in a mammalian phosphodiesterase. J Biol Chem 1999; 274: 4839-47.

[81] Herman SB, Juilfs DM, Fauman EB, Juneau P, Menetski JP. Analysis of a mutation in phosphodiesterase type 4 that alters both

inhibitor activity and nucleotide selectivity. Mol Pharmacol 2000; 57: 991-9.

[82] Richter W, Unciuleac L, Hermsdorf T, Kronbach T, Dettmer D. Identification of substrate specificity determinants in human cAMP specific phosphodiesterase 4A by single-point mutagenesis. Cell Signal 2001; 13: 159-67.

[83] Wade RC, Henrich S, Wang T. Using 3D protein structures to derive 3D-QSARs. Drug Discov Today Tech 2004; 1: 241-46.

[84] Srivani P, Kiran K, Sastry GN. Understanding the structural requirements of triarylethane analogues towards PDE-IV inhibitors: A molecular modeling study. Ind J Chem A 2006; 45A: 68-76.

[85] Srivani P, Srinivas E, Raghu R, Sastry GN. Molecular modeling studies of pyridopurinone derivatives - Potential phosphodiesterase5 inhibitors. J Mol Graph Model 2007; 26: 378-90.

[86] Kulkarni GK, Srivani P, Achiah G, Sastry GN. Strategies to design pyrazolyl urea derivatives for p38 kinase inhibition: A molecular modeling study. J Comp Aided Mol Des 2007; 21: 155-66.

[87] Ochiai H, Ishida A, Ohtani T, Kusumi K, Kishikawa K, Obata T, *et al.* New orally active PDE4 inhibitors with therapeutic potential. Bioorg Med Chem Lett 2004; 14: 29-32.

[88] a) Buckley GM, Cooper N, Dyke HJ, Galleway FP, Gowers L, Haughan AF, *et al.* 8-Methoxyquinoline-5-carboxamides as PDE4 inhibitors: A potential treatment for asthma. Bioorg Med Chem Lett 2002; 12: 1613-5. b) Billah M, Buckley GM, Cooper N, Dyke HJ, Egan R, Ganguly A, *et al.* 8-Methoxyquinolines as PDE4 inhibitors. Bioorg Med Chem Lett 2002; 12: 1617-1619. c) Gallant M, Chauret N, Claveau D, Day S, Deschênes D, Dubé D, *et al.* Design, synthesis, and biological evaluation of 8-biarylquinolines: A novel class of PDE4 inhibitors. Bioorg Med Chem Lett 2008; 18:1407-12.

[89] Buckley GM, Cooper N, Richard JD, Dyke HJ, Galleway FP, Gowers L, *et al.* 7-Methoxyfuro[2,3-c]pyridine-4-carboxamides as PDE4 Inhibitors: A potential treatment for asthma. Bioorg Med Chem Lett 2002; 12: 509-12. b) Buckley GM, Cooper N, Dyke HJ, Galleway FP, Gowers L, Galleway F, *et al.* 7-Methoxybenzofuran-4-carboxamides as PDE 4 Inhibitors: A potential treatment for asthma. Bioorg Med Chem Lett 2000; 10: 2137-40.

[90] Ochiai H, Odagaki Y, Ohtani T, Ishida A, Kusumi K, Kishikawa K, *et al.* Design, synthesis, and biological evaluation of new phosphodiesterase type 4 inhibitors. Bioorg Med Chem 2004; 12: 5063-78. b) Kim E, Chun H-O, Jung S-H, Kim JH, Lee J-M, Suh B-C, *et al.* Improvement of therapeutic index of phosphodiesterase type IV inhibitors as anti-asthmatics. Bioorg Med Chem Lett 2003; 13: 2355-8.

[91] Pascal Y, Andrianjara CR, Auclair E, Avenel N, Bertin B, Calvet A, *et al.* Synthesis and structure activity relationships of 4-Oxo-1-phenyl-3,4,6,7-tetrahydro-[1,4]diazepino[6,7,1-hi]indoles: Novel PDE4 inhibitors. Bioorg Med Chem Lett 2000; 10: 35-8.

[92] Whitehead JWF, Lee GP, Gharagozloo P, Hofer P, Gehrig A, Wintergerst P, *et al.* 8-Substituted analogues of 3-(3-Cyclopentyloxy-4-methoxy-benzyl)-8-isopropyladenine: Highly potent and selective PDE4 inhibitors. J Med Chem 2005; 48: 1237-43.

[93] Kuang R, Shue Ho-J, Blythin DJ, Shih NY, Gu D, Chen X, *et al.* Discovery of a highly potent series of oxazole-based phosphodiesterase 4 inhibitors. Bioorg Med Chem Lett 2007; 17: 5150-4.

[94] Skoumbourdis AP, Huang R, Southall N, Leister W, Guo V, Cho M-H, *et al.* Identification of a potent new chemotype for the selective inhibition of PDE4. Bioorg Med Chem Lett 2008; 18: 1297-303.

[95] Chakraborti AK, Gopalakrishnan B, Sobhia ME, Malde A. 3D-QSAR studies on thienol[3,2-*d*]pyrimidines as phosphodiesterase IV inhibitors. Bioorg Med Chem Lett 2003; 13: 1403-8.

[96] Chakraborti AK, Gopalakrishnan B, Sobhia ME, Malde A. 3D-QSAR studies of indole derivatives as phosphodiesterase IV inhibitors. Bioorg Med Chem Lett 2003; 38: 975-82.

[97] Guay D, Hamel P, Blouin M, Brideau C, Chan CC, Chauret N, *et al.* Discovery of L-791, 943: A potent, selective, non-emetic and orally active phosphodiesterase-4 inhibitor. Bioorg Med Chem Lett 2002; 12; 1457-61.

[98] Graves AP, Brenk R, Shoichet BK. Decoys for docking. J Med Chem 2005; 48: 3714-28.

[99] Xu RX Hassell AM, Vanderwall D, Lambert MH, Holmes WD, Luthe MA, *et al.* Atomic structure of PDE4: Insight into phosphodiesterase mechanism and specificity. Science 2000; 288: 1822-5.

[100] Dym O, Xenarios I, Ke H, Colicelli J. Molecular docking of competitive phosphodiesterase inhibitors. Mol Pharmacol 2002; 61: 20-5.

[101] Piaz DV, Giovannonia MP, Castellana C, Palacios JM, Beleta J, Doménech T, *et al.* Heterocyclic-fused 3(2H)-pyridazinones as potent and selective PDE IV inhibitors: Further structure-activity relationships and molecular modelling studies. Eur J Med Chem 1998; 33: 789-97.

[102] Mpamhanga CP, Chen B, McLay IM, Ormsby DL, Lindvall MK. Retrospective docking study of PDE4B ligands and an analysis of the behavior of selected scoring functions. J Chem Inf Model 2005; 45: 1061-74.

[103] Oliveira FG, Sant'Anna CMR, Caffarena ER, Dardenne LE, Barreiro EJ. Molecular docking study and development of an empirical binding free energy model for phosphodiesterase 4 inhibitors. Bioorg Med Chem 2006; 14: 6001-11.

[104] a) Lawrenz ME, Salter EA, Wierzbicki A, Thompson WJ. Molecular modeling study of binding to the catalytic site of PDE4 enzymes by a novel class of inhibitors. Int J Quantum Chem 2005; 105: 410-5. b) Tait A, Luppi A, Hatzelmann A, Fossa P, Mosti L. Synthesis, biological evaluation and molecular modeling studies on benzothiadiazine derivatives as PDE4 selective inhibitors. Bioorg Med Chem 2005; 13: 1393-402.

[105] Jeon JH, Heo Y-S, Kim CM, Hyun Y-L, Lee TG, Ro S, Cho JM. Phosphodiesterase: Overview of protein structures, potential therapeutic applications and recent progress in drug development. Cell Mol Life Sci 2005; 62: 1198-220.

[106] Ke H, Wang H. Crystal structures of phosphodiesterases and implications on substrate specificity and inhibitor selectivity. Curr Top Med Chem 2007; 7: 391-403.

[107] Wang H, Peng M, Chen Y, Geng J, Robinson H, Houslay MD, *et al.* Structures of the four subfamilies of phosphodiesterase-4 provide Insight into the selectivity of their Inhibitors. Biochem J 2007; 408: 193-201.

[108] Lee ME, Markowitz J, Lee JO, Lee H. Crystal structure of phosphodiesterase 4D and inhibitor complex. FEBS Lett 2002; 530: 53-8.

[109] Huai Q, Colicelli J, Ke H. The crystal structure of AMP-bound PDE4 suggests a mechanism for phosphodiesterase catalysis. Biochemistry 2003; 42: 13220-6.

[110] Zhang KYJ, Card GL, Suzuki Y, Artis DR, Fong D, Gillette S, *et al.* A glutamine switch mechanism for nucleotide selectivity by phosphodiesterases. Mol Cell 2004; 15: 279-86.

[111] Card GL, England BP, Suzuki Y, Fong D, Powell B, Lee B, *et al.* Structural basis for the activity of drugs that inhibit phosphodiesterases. Structure 2004; 12: 2233-47.

[112] Card GL, Blasdel L, England BP, Zhang C, Suzuki Y, Gillette S, *et al.* A family of phosphodiesterase inhibitors discovered by cocrystallography and scaffold-based drug design. Nat Biotechnol 2005; 23: 201-7.

[113] Huai Q, Sun Y, Wang H, Macdonald D, Aspiotis R, Robinson H, *et al.* Enantiomer discrimination illustrated by the high resolution crystal structures of type 4 phosphodiesterase. J Med Chem 2006; 49: 1867-73.

[114] Wang H, Liu Y, Huai Q, Cai J, Zoraghi R, Francis SH, *et al.* Multiple conformations of PDE5. J Bio Chem 2006; 281: 21469-79.

[115] Sapse, A-M. Molecular orbital calculations for amino acids and peptides. Birkhaüser, boston, MA, 2000.

[116] MOE version 2006 Chemical Computing Group, 954, First Floor, 16th Main, BTM Layout 2nd Stage, Bangalore, India 560 076.

[117] Bindu PH, Sastry GM, Murty USN, Sastry GN. Structural and conformational changes concomitant with the E1-E2 transition in H^+K^+-ATPase: A comparative protein modeling study. Biochem Biophys Res Commun 2004; 319: 312-20.

[118] Manallack DT, Hughes RA, Thompson PE. The next generation of phosphodiesterase inhibitors: Structural clues to ligand and substrate selectivity of phosphodiesterases. J Med Chem 2005; 48: 1-14.

[119] a) Genchek™ copyright 2000-2006 Ocimum biosolutions. b) Kyte J, Doolittle, RF. A simple method for displaying the hydropathic character of a protein, J Mol Biol 1982; 157: 105-32.

[120] a) Connolly ML. Solvent accessible surfaces of proteins and nucleic acids. Science 1983; 221: 709-713. b) Connolly ML. Analytical molecular surface calculation. J Appl Crystallogr 1983; 16: 548-58.

[121] a) Ghose AK, Crippen GM. Atomic physicochemical parameters for three-dimensional structure directed quantitative structure-activity relationships I: Partition coefficients as a measure of hydrophobicity. J Comp Chem 1986; 7: 565-77. b) Ghose AK, Pritchett A, Crippen GM. Atomic physicochemical parameters for three-dimensional structure directed quantitative structure-activity relationships III: Modeling hydrophobic interactions. J Comp Chem 1988; 9: 80-90.